ENERGY LOSS OF
HIGH ENERGY ELECTRONS

A THESIS

PRESENTED TO

THE FACULTY OF GRADUATE STUDIES

UNIVERSITY OF MANITOBA

IN PARTIAL FULFILLMENT

OF THE REQUIREMENTS FOR THE DEGREE

MASTER OF SCIENCE

---

by

THOMAS C. OLIEN

OCTOBER, 1966

ACKNOWLEDGEMENTS

The research described in this thesis was carried out at The Manitoba Cancer Treatment and Research Foundation under the supervision of Dr. A. F. Holloway. His guidance and the assistance from the staff of the Physics Department of The Manitoba Cancer Treatment and Research Foundation is gratefully acknowledged.

The assistance, through the provision of a calibration source and instruction in the operation of a semiconductor detector system, given by Dr. S. K. Sen of the Physics Department of The University of Manitoba; and the insight into the question of energy dissipations by electrons given by Dr. D. V. Cormack of the Physics Department of The University of Saskatchewan, is acknowledged.

The financial assistance provided by The Manitoba Cancer Treatment and Research Foundation is much appreciated.

ENERGY LOSS OF
HIGH ENERGY ELECTRONS

THOMAS C. OLIEN

ABSTRACT

A survey of the topics concerned with the energy loss of high energy electrons revealed several areas where major questions as yet remain unanswered. One such area was the relative biological effectiveness of electrons. A controversy existed on the question of a change in the relative biological effectiveness of electrons with depth in an absorbing medium.

An investigation was made to determine the nature of the information available from a semiconductor detector when placed in a beam of high energy electrons. Measurements were made with the detector at various depths in lucite.

Two detectors were used. One was a silicon, fully depleted, surface barrier detector, 450 microns thick; the other was a silicon, fully depleted,multi-diffused junction detector, 220 microns thick. High energy electrons were not stopped in either of these detectors but deposited a small amount of energy as they passed through the detector. The current pulse produced by such an energy deposition was amplified by a charge-sensitive preamplifier, further amplified by a pulse shaping amplifier, and then analyzed

by a pulse height analyzer. Using a betatron as the source of high energy electrons, a spectrum of the energy depositions of single electrons traversing a detector was accumulated by the pulse height analyzer.

From the two detectors, energy dissipation spectra due to 20 MeV and 35 MeV electrons were obtained for various depths in lucite. The results revealed a very prominent peak for the most probable energy loss, and a mean energy loss lower than the energy loss calculated from the mean stopping power times the thickness of the detector. These results were explained by theoretical calculations. With increasing depths in the absorber a greater number of higher energy depositions occurred. Two possible causes of this variation with depth were given, although it could not be determined which cause was responsible for the effect. One possible cause was secondary electrons of energy less than 1 MeV. A build-up of such secondary electrons with depth leads to an increasing relative biological effectiveness with depth. Suggestions were given as to how semiconductor detectors could further be used to obtain information on such questions.

TABLE OF CONTENTS

LIST OF TABLES

LIST OF FIGURES

CHAPTER I

INTRODUCTION

From its earliest introduction, radiation has been used on biological organisms, including human beings. For instance, X-rays were successfully used for tumor treatment in 1899. However, it often took days before any observable reaction to the radiation could be recorded, in spite of the fact that such reactions must have been initiated at the time of irradiation. Dosimetry, i.e. the questions of quality of radiation and of rate of delivery, often had to be based on these delayed clinical results. Nevertheless, the aim has always been to develop physical, chemical, or other than human biological means of dosimetry that would in turn allow reliable predictions of clinical results.

The standardization of X-ray dose by the introduction of the roentgen was an important step in the desired direction. An X-ray dose of a given number of roentgens in a given clinical application gave reproducible results that became well known and served as a basis for predicting results in unknown applications. However, the roentgen was defined in terms of medium voltage X-rays, and the measuring equipment of the time. The introduction of higher voltage X-rays, gamma rays, and then especially electrons, protons, and neutrons has raised new

questions for the fields of dosimetry and radiobiology. Physically the problem has been to determine by experiment, or calculation, the total energy and distribution of energy deposited by a variety of radiations in a variety of media. This has demanded increased precision not only in measurement techniques but also in the qualitative and quantitative description of the interaction mechanisms. Biologically the problem has been to determine the fundamental biological effects associated with a sudden deposit of energy. The aim has been to relate a given pattern of energy deposits with particular biological effects. Much remains to be done before it is possible to answer these questions completely, and to realize the goal of reliable predictions of clinical results from all radiations.

In particular, there has been controversy over the biological effect of high energy electrons. Some experiments have suggested a depth dependence in the biological effectiveness of such radiation while other experiments indicate no variation with depth. Most hypotheses on the mechanism by which an energetic electron produces a biological change agree that secondary electrons play the most important role. Calculations of the secondary electron spectrum and its variations with depth have not all agreed. Not a great deal of experimental information about the secondary electron spectrum has been obtained. It was in response to this

need for further experimental information on the energy loss of high energy electrons that the project reported in this thesis was undertaken.

Semiconductor detectors presented a potentially new source for information on the energy loss of electrons. The purpose of this project was to determine what information might be obtained from these detectors, in particular, with respect to variations of energy loss with depth in an absorbing medium.

The source of electrons was a 35 MeV betatron installed at The Manitoba Cancer Treatment and Research Foundation. Although this betatron is used daily in therapeutic treatment, it has been the desire of the Physics Department of The Manitoba Cancer Treatment and Research Foundation that other scientific uses of the betatron be explored. Thus a secondary purpose of this project has been to adapt the betatron from routine operation in an application other than therapy.

Chapter II will introduce the concepts involved in describing the interaction of a beam of high energy electrons with matter. Some of the problems related to the use of such a source of radiation will be discussed. Chapter III will describe the operation of the betatron, the semiconductor detector, and other experimental equipment used in the project. The methods for collecting and

analyzing the data are to be presented in Chapter IV. These results will be compared to theoretical predictions and their implications will be discussed in Chapter V. Chapter VI will present the conclusions that can be drawn from the experimental work. Suggestions for further experimental work will also be included in Chapter VI.

CHAPTER II

HIGH ENERGY ELECTRONS

Electrons of energies in the range of 3 MeV to 100 MeV are arbitrarily referred to as high energy electrons [1]. The main sources of such electrons, as used for radiotherapy, include electrostatic generators, resonant transformers, linear accelerators, betatrons and synchrotrons [1,2]. Widespread and imaginative use of such machines has produced valuable clinical information. Nevertheless there is still the desire to understand just what takes place when high energy electrons penetrate materials of low atomic number. The "Symposium on High Energy Electrons" which convened in Montreux, Switzerland, September 1964, is an indication of the magnitude and urgency of the questions associated with routine use of high energy electrons.

It is convenient to consider four areas in which advancement has been made and continues to be made. The four areas are: (1) the basic interactions of electrons with matter, (2) the macroscopic concepts of dose, dose rate, depth dose, and energy spectra, (3) the microscopic aspects of energy transfer to the media, and, (4) the relative biological effectiveness of electron radiations. This chapter is an elaboration on these four aspects of the passage of a beam of high energy electrons through

matter.

A. INTERACTIONS OF ELECTRONS WITH MATTER

Several mechanisms are involved in the interaction of an electron with matter. Those that pertain to the stopping of high energy electrons include inelastic collisions with atomic electrons resulting in primary ionization, elastic collisions with atomic electrons producing secondary electrons, elastic scatter off atomic nuclei, and radiative collisions with atomic nuclei, i.e. the Bremsstrahlung emission. The relative importance of these interactions varies with different materials and with the energy of the electron. Thus there is no simple expression for describing these variations over any significant range of materials or energies.

Considerable theoretical work has been done to clarify the qualitative and quantitative details of the above reactions. The outcome of this work is conveniently assembled in texts such as those by H. Bethe and J. Ashkin [3], R. D. Evans [4], and R. D. Birkhoff [5]. Clarification of the importance of secondary electrons has been given by L. V. Spencer and H. H. Attix [6], and P. J. R. Burch [7]. R. M. Sternheimer [8,9,10] evaluated the density effect on ionization losses in various materials.

With the availability of computer facilities elaborate tables of the theoretical calculations over wide ranges of materials and energies have been produced. A. Nelms [11] tabled the range and energy loss of electrons and positrons with energies up to only a few MeV so that Bremsstrahlung losses could be neglected. The most complete tables to date of energy losses and ranges of electrons and positrons are given by M. J. Berger and S. M. Seltzer [12]. They have tables for forty materials including organic compounds, muscle, bone, air and standard emulsion, with electron energies from 10 keV to 1000 MeV. Collisional and radiation losses are given separately and the total radiation yield in stopping the electron is shown. Other properties such as the energy spectrum produced by electrons slowing down as tabled by R. T. McGinnies [13], and the energy dissipated at different distances by monoenergetic electron sources up to 10 MeV as tabled by L. V. Spencer [14], now allow the experimenter or clinician to make a wide variety of specific calculations and predictions.

The specific equations required for calculations in this project are discussed in Appendix A. It is sufficient at this point to present a descriptive picture of the interactions of interest.

Consider the electrons numbered one to ten in Figure 1. Let them be monoenergetic and normally

FIGURE 1

INTERACTIONS OF ELECTRONS WITH MATTER

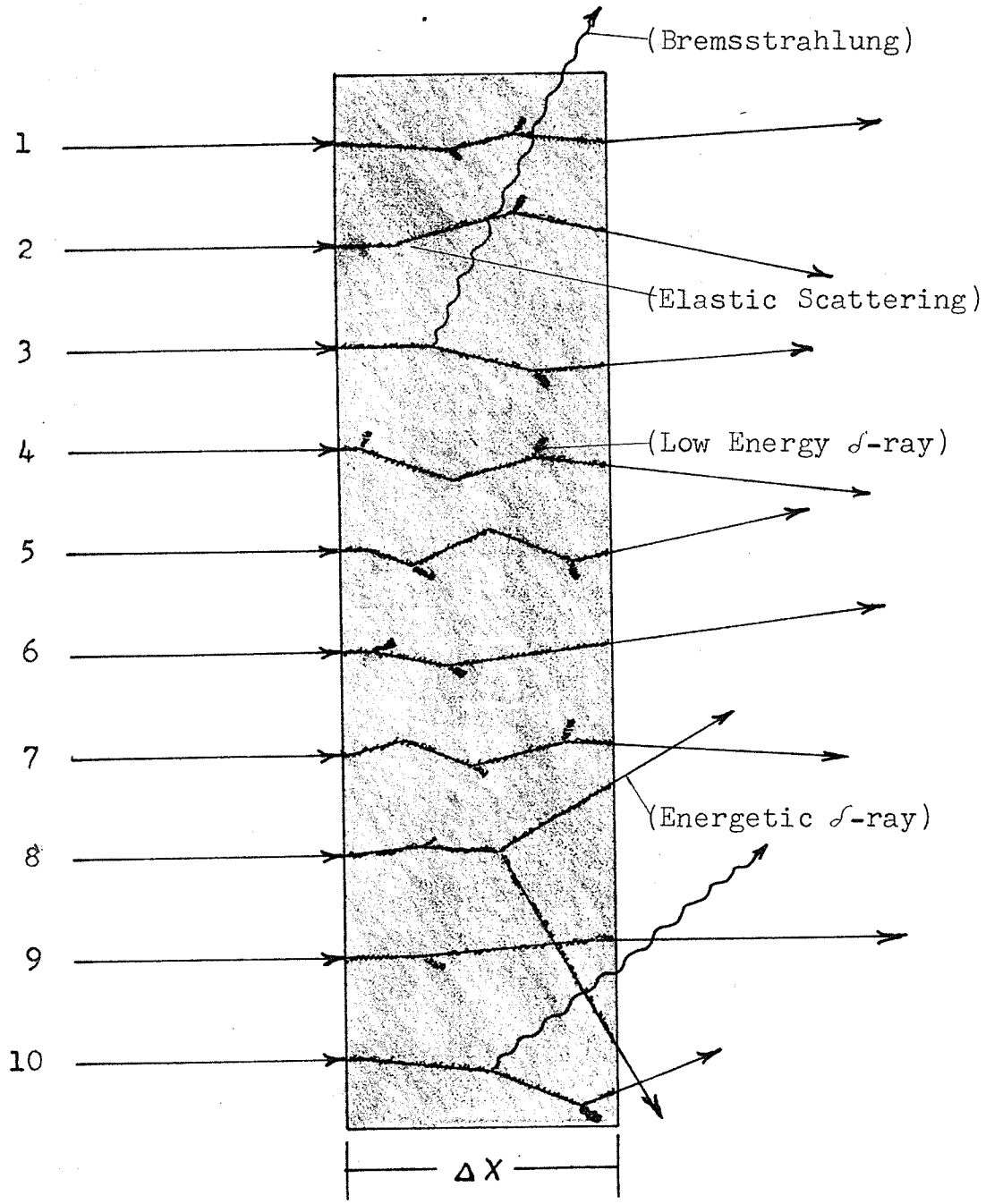

(INCIDENT) (ABSORBING) (EMERGENT)

(ELECTRON) (MEDIUM) (ELECTRON)

incident to the thin slab of material of thickness Δx. All electrons will immediately begin to excite and ionize the atoms of the material. These are the inelastic collisions with atomic electrons which result in primary ionization. In fact, except for very high energy electrons, these inelastic collisions are the major means by which the energy of an electron is lost. Very little energy is lost in a given single interaction since excitations involve only tens of electron volts, and ionizations a few hundreds of electron volts. It is the large number of such interactions that makes their contribution significant. If these were the only interactions, the electron would slow down continuously in a very predictable manner. There would be a well defined average loss per unit distance, a relatively straight path and thus a well defined range for the electron. This is the case for heavier particles such as protons or alphas of moderate energy.

However, considerably more than just the average ionization energy can be transferred to an atomic electron. In fact, the energetic electron in a head-on collision could transfer its total energy to an atomic electron. But, since there is no way of knowing which electron is which, the one with the highest energy after the collision is taken to be the primary electron. The

other is the secondary electron, and thus by definition can have up to one half the energy of the original energetic electron. If the ejected secondary electron itself has sufficient kinetic energy to cause further ionization, this secondary electron may be called a delta (δ) ray. If the average ionization potential can be neglected compared to the energy transferred, the collision producing the secondary electron can be considered to be an elastic collision with an atomic electron.

The cross-section for delta ray production varies approximately inversely with the energy of the delta ray. Thus only a few large energy exchanges occur, while a great number of delta rays are produced with merely enough energy to cause a few ionizations close to the primary track. Compare electron #8 with electrons #1,2,4,5,6,7,9 in Figure 1. Note, however, that electron #8 has lost a large fraction of its energy in such a collision. Thus although their probability is small, high energy exchanges contribute significantly to the energy loss of the primary electron. Also, since there are now two electrons ionizing instead of one, the number of ions produced in a given volume will be much greater. Consider a thin slab of material, such that the probability of a high energy transfer within its volume is very small. There will then be a significant difference between the most probable

energy loss that occurs and the average energy loss that is predicted for electrons.

It is to be noted that in the case of electron #8, energy is being carried off in a different direction to a region some distance away from the initial path of the primary electron. Thus, although the primary electron has suffered a large energy loss, very little of this has been deposited locally. This introduces the concept of linear energy transfer, defined in N.B.S. Handbook 84 [15], as the average energy locally imparted to the medium per unit distance travelled by the primary particle. The region local to the primary must be specified, but is chosen arbitrarily. It may be in terms of a maximum distance from the primary track or a maximum discrete energy loss by the primary above which the loss is no longer considered as local.

Figure 1 illustrates another feature of the interaction of an electron with matter. The path of the electron is poorly defined. In the production of delta rays the primary electron may be deflected up to 45° when it transfers half of its energy to a secondary. Many smaller deflections take place as lower energy delta rays are produced.

Electrons may undergo elastic scatter off atomic

nuclei. Electrons #2,4,5,7,9 show such interactions. In this case the mass of the nucleus is so much greater than that of the electron, that negligible amounts of energy are transferred to the nucleus. Thus the path of the electron may be significantly altered without any energy loss. If such scattering takes place many times over the distance of observation the actual path length required to stop the electron will seldom correspond to the range of penetration of the particle. The range may be considerably less than the stopping path length, or equivalently the rate of energy loss per unit thickness may be greater than predicted.

The fourth mechanism of electron interaction is illustrated by electrons #3 and #10 in Figure 1. This is the radiative collision with an atomic nucleus. An energetic electron can be decelerated by an atomic nucleus and classical theory demands that whenever a charge undergoes a deceleration, it must radiate. In contrast quantum mechanical theory claims that there is a small but finite probability that a deceleration can take place, followed by the emission of a quantum of radiation. The rest of the time no energy is transferred in the interaction. Thus most interactions of the electron with the nucleus result in elastic scatter as mentioned above, and occasionally a photon is created. Although radiative collisions may be

less frequent than elastic collisions, they do play a significant role in the energy loss of electrons, because a large fraction of the energy of an electron can be transferred in the radiative interaction. The energy transferred to the photon is not deposited until the photon is absorbed at some distance from its origin. In any beam of high energy electrons an associated field of Bremsstrahlung radiation develops. The reabsorption of this radiation can be considered as another source of energy and accounts for the energy deposition beyond the maximum range of the electrons.

The occurrence of Bremsstrahlung radiation makes little difference to the energy deposited in the region local to the high energy electron primary. Ionization has taken place up to the point of the radiative collision and in most cases the electron retains sufficient energy after the interaction to continue ionizing at about the same rate. Self-absorption of a photon created within a small volume is very unlikely, and so there is no local contribution to energy deposition by the photon.

This descriptive picture of the interactions of individual electrons with matter serves as a basis for understanding what takes place when a beam of particles passes through matter. The relative importance of each

of these individual interactions together with the large number of interactions gives the beam its characteristic pattern of penetration in matter.

B. MACROSCOPIC CONCEPTS OF DOSE AND RELATED PHENOMENA

In dealing with a beam of electrons in which the individual electrons are undergoing the interactions discussed above, there are several macroscopic concepts that must be introduced. One is concerned with the rate at which energy is delivered to the media and the rate at which it is absorbed. The pattern of the energy absorption and the quality of the radiation that is depositing the energy at a given point are also questions of interest. These questions are discussed in this section.

The intensity of the beam is the total kinetic energy of all the particles passing through a unit area per unit time. This quantity should be measured by a calorimeter, in which the particles are completely brought to rest, or if the energy of the electrons is known, by a Faraday Cup which will tell the total number of such electrons per unit time. In practice a transmission ion chamber is often used. The ion density produced and collected can be related to the intensity of a beam of

known electron energy [1].

The next quantity of interest is the amount of energy absorbed by the media. This is the absorbed dose, defined in N.B.S. Handbook 84 [15] as the energy imparted to matter by ionizing radiation per unit mass. The special unit for absorbed dose, or simply "dose" when its context is properly understood, is the rad which is equal to 100 ergs per gram. Among the many ways to measure this quantity, including calorimetry, chemical means, and photographical techniques, the ionization chamber is one of the most common methods. In the ion chamber itself the dose is given by:

$$D_I = J \frac{w}{e} \times 1.6 \times 10^{-12} \quad \ldots\ldots\ldots\ldots\ldots\ldots\ldots\ldots (1)$$

where
- D_I is the absorbed dose in the ion chamber in ergs/gm
- J is the charge collected in coulombs per gram of air in chamber
- w is the average energy required to produce one ion pair in air and the currently accepted value is 33.7 electron volts per ion pair
- e is the charge per ion pair in coulombs
- the factor 1.6×10^{-12} is the conversion factor from electron volts to ergs.

The classic question in the development of radiation dosimetry is the relationship of the absorbed dose in the

ionization chamber to the absorbed dose in the medium of interest. This question was first asked in conjunction with X-ray dosimetry, and was answered formally in the Bragg-Gray principle: [16,17,18]

$$E_a = \frac{1}{s} E_m \quad \text{.....(2)}$$

where - E_a and E_m are the energies lost by electrons per cubic centimeter in traversing air and the medium of interest respectively

- s is a proportionality factor

Gray claimed s to be independent of the velocity of the particle and identified it as the ratio of the stopping power in the solid media to that in air. Although the principle remains, it has had to undergo many refinements. G. C. Laurence [19] restated the problem using a different model and took into account the effect of the walls and the energy dependence of the stopping power ratio. A refinement to Laurence's model was added by G. N. Whyte [20] as he considered the polarization effect in solid materials. Finally, L. V. Spencer and F. H. Attix [6], and P. J. R. Burch [7,21] presented almost simultaneous, but independent formulations of the Bragg-Gray principle which included close analysis of the effects of the secondary electrons. Their presentations represent the most complete theoretical consideration on

the subject of cavity ion chambers to date and a variety of experiments have tested their theory to a high degree of accuracy over a wide range of conditions [22,23]. A very complete work on the theory and use of cavity chambers is N.B.S. Handbook 79 [24].

For applying the ionization chamber on a regular basis to the dosimetry of fast electrons Dietrich Harder derived some very useful results [25]. The Bragg-Gray relation for a beam of electrons incident on a medium m and being monitored by an air filled ion chamber is given as:

$$D_m = J_a \frac{W}{e} r \quad \ldots\ldots\ldots\ldots\ldots\ldots\ldots\ldots\ldots\ldots\ldots\ldots (3)$$

where - r is an energy-dependent conversion factor

- the other symbols are as previously defined

The conversion factor r is the ratio of the mass stopping powers at the energy E of the electrons. However, a monoenergetic beam will not remain monoenergetic for long, but will assume an energy spectrum which is dependent on depth of penetration. The spectrum will include the build-up of secondary electrons, as well as the degradation of the primary electrons. To define r so as to include all these effects would be extremely complicated, but it is shown by Harder that if the secondary electron flux is at

equilibrium, the secondaries can be ignored in the calculation of r. He then shows that within the desired degree of accuracy, a secondary electron equilibrium does exist and r becomes simply the relative mass stopping powers for the primary electrons. In a second paper by Harder [26], on the energy spectrum of fast electrons at different depths, it is shown by experiment and calculations that for low atomic number materials the mean electron energy decreases linearly with depth and thus can be represented by:

$$E_m = E_a \left(1 - \frac{d}{R_p} \right) \quad \ldots\ldots\ldots\ldots\ldots\ldots\ldots\ldots (4)$$

where
- E_m is the mean electron energy at depth d
- E_a is the incident electron energy
- d is the depth in absorbing material
- R_p is the practical range in this material.

If one represents the energy spectrum at a depth by the mean energy as calculated above and combines this with the energy dependence of the ratio of mass stopping powers one can get the depth dependence of this ratio. Assuming secondary electron equilibrium, this is also the value for r in equation (3). Experimental checks on the procedure revealed an accuracy of 2% for energies up to 50 MeV in low atomic number materials. Thus, Harder concludes that it is possible to reliably and conveniently

measure the absorbed dose due to a beam of high energy electrons by means of ionization chambers.

One is then lead to the question of the macroscopic distribution of the dose delivered by an electron beam to a given medium. Photographic film can conveniently yield the relative dose distribution and with extreme care may be used to measure absolute dose. More often a Fricke ferrous sulfate chemical dosimeter, an ion chamber or some other dosimeter is used to measure the absolute dose at a given point in the distribution and thus calibrate the film. In practice the film is surrounded by the medium of interest and positioned to record the desired cross section of the electron beam. The standard procedure is to sandwich the film in the layers of a tissue-equivalent phantom, positioned along the central axis of the beam and in the orbital plane of the betatron. When such a film is developed and the optical density converted to relative dose one can construct an isodose pattern of the dose distribution.

The field size is determined by a set of lucite collimators and special patterns can be obtained with filters, magnetic focusing and other techniques. Depth of penetration by the beam is primarily controlled by the initial energy of the electrons. Central axis depth dose curves are another common means of relating information

about the dose distribution and are particularly useful for indicating the depth of penetration of a beam. Examples of isodose patterns and depth dose curves are included in a paper on the properties of high energy electrons by J. W. Beattie et al [27]. Due to the relatively constant rate of energy loss by fast electrons over most of their range, the dose distribution from an electron beam features a large volume over which a high relative dose can be maintained, with a sharp cutoff at the sides and maximum range of the beam. By use of the proper field-size collimator and energy of the electron beam, considerable control of the dose distribution may be exercised.

The betatron beam is monitored by a thin-walled transmission ionization chamber with instantaneous and integrated output indicated. This monitor has been correlated with the absolute absorbed dose in the region of 100% relative dose for all field size and energies. Thus one is able to determine the macroscopic absorbed dose for any position in the radiated region.

The last macroscopic concept to be mentioned is the variation of the <u>electron energy spectrum</u> with depth. This is mentioned by G. W. Dolphin et al [27] in their discussion of the operation of a 15 MeV linear accelerator. By the Monte-Carlo method, Harder [26] calculates the energy spectrum for depths in carbon and confirms his calculations

by experiment. Both these investigators find that the mean energy decreases linearly with depth in the absorber, and that the spectrum broadens with an increasing low energy tail. Little information is given in their work on the energy spectrum of the secondary electrons. Since the primary spectrum and the secondary electron production cross-section are known one should be able to calculate the secondary electron spectrum. Nevertheless, it would be of value if this spectrum could be seen experimentally. This was one of the questions which initially prompted interest in semiconductor detectors for the study of electron interactions. However, of even greater interest were some of the microscopic aspects of the interaction of a fast electron with matter.

C. MICROSCOPIC ASPECTS OF ENERGY TRANSFER TO THE MEDIUM

To understand the fundamental changes that take place when biological materials are irradiated, it is necessary to bridge the gap between the atomic interaction and the macroscopic measurement of the total energy deposited in the volume of material. The role of secondary electrons and the concept of linear energy transfer are two factors that arise when one considers this gap.

It was early recognized that the production of

secondary electrons was involved in the interaction of an energetic electron with matter. By 1932, N. F. Mott [29] and C. Moller [30] had developed cross sections for secondary electron production from non-relativistic and relativistic primaries. These expressions were tested thoroughly and were found reliable within experimental error. However, only recently have the secondary electrons been brought to the foreground. As mentioned above, it was not until 1955 that Spencer and Attix and then Burch presented cavity ion chamber theories that recognized the special effects due to the production of a few high energy secondaries. At about the same time, interest in the energy deposition by ionizing particles at the local level was increasing as it was realized that this was the key to the biological effect of the radiation.

Mean ion densities from X-rays generated at 10 to 1000 kVp were published by L. H. Gray [31]. By first determining the primary electron spectrum due to 200 keV X-rays, Co^{60} γ rays, and 25 MeV X-rays, D. V. Cormack and H. E. Johns [32] were able to calculate the ion density spectra due to the primary electron from these radiations. R. E. Zirkle et al [33] introduced the idea of linear energy transfer, LET, (defined earlier in the chapter) which took into account the energy loss in excitation as well as ionization. But again, P. J. R. Burch [34, 35], was the one

who devised a method of calculating a mean LET that would take into account the effect of the secondary electrons. He calculated results for X-rays from 200 keV to 25 MeV as well as for tritium beta-particles and two energies of α particles. R. H. Haynes and G. W. Dolphin [36] applied Burch's method of calculating a local energy dissipation spectrum to 14 MeV electrons in water. Considering only secondary electrons below 100 eV as local, they also produced a spectrum of energy dissipated per log LET interval versus log LET. From this, one could determine the amount of energy that was being deposited in any LET interval, and it was found that most of the energy was produced in the higher LET region, i.e. due to the large number of secondaries with high LET. A mean LET was also determined from the energy dissipation versus LET spectrum. To assign any absolute significance to this number was difficult but it did give some basis for comparing different radiations in a quantitative way. The authors also decided that one such comparison could be the variation of mean LET with depth in the media. They argued that there was an extremely small mean LET at the surface and this rapidly rose to a plateau level that applied to most of the path of the electron. At the end of the path there was a rise in mean LET, and then it fell to zero as the electron stopped.

Further discussion of the role of the secondary electrons and the usefulness of the LET concept will be found under the heading of relative biological effectiveness. It has been shown that there is now a strong interest in the part that secondary electrons play in the stopping of a high energy electron. Cross sections are available for calculating the spectrum of secondary electrons produced by a known primary spectrum. One can also calculate an ion density or LET spectrum. However, it is not yet known what takes place when a passing electron has a kinetic energy of the same order as the energy of the atomic electrons. This is clearly stated by U. Fano as one of the currently unsolved problems related to the penetration of charged particles in matter [37].

> No opportunity exists within the first Born approximation to extend the theory of electron collisions down to incident velocities comparable to those of atomic electrons, that is, to proceed by analogy with the shell corrections in heavy particle collision theory. No realistic suggestion is known to this writer concerning methods for a basic attack on the stopping power of slower electrons and positrons. Here again a survey study might be profitable - to assess the relevant aspects of the problem and their presumable influence on stopping power.

As will be shown later, the suggestion is that at precisely such energies, electrons produce their greatest, if not their

only biological effect.

D. RELATIVE BIOLOGICAL EFFECTIVENESS

In less than a century the list of radiations known to man has grown from the X-rays of Roentgen and radioactive particles of Becquerel, to include higher energy photons, electrons, positrons, protons, neutrons, alpha particles and a whole variety of ions, and now even an expanding catalogue of elementary particles. This variety has posed a series of questions for those involved in the fields of radiation protection, radiotherapy, and radiobiology. The first question was that of dosimetry: i.e. measurement of the energy deposited macroscopically in a given medium by one of the above radiations. The second question was that of relative biological effectiveness, as it was soon discovered that equal doses of different radiations did not necessarily have the same effect on biological organisms. Dosimetry, as required for electrons, has been discussed previously. Similar problems, and similar solutions, apply to the other radiations as well. Relative biological effectiveness, or RBE, in its strict sense is a rather complex function. Not only is there a relative effectiveness among different types of radiations, but for two given radiations, their

relative effectiveness is further dependent on the nature of the biological effect being considered, as well as in some cases, the dose rate. Thus the strict definition of RBE, as given in the Report of the RBE Committee to the ICRP and ICRU is:

$$\text{RBE } \left(\frac{t}{s}, u\right) = \frac{D_s \ (u)}{D_t \ (u)} \quad \ldots\ldots\ldots\ldots\ldots\ldots\ldots\ldots (5)$$

This is interpreted to mean that the relative biological effectiveness of a test radiation t as compared to a standard radiation s for producing the particular qualitative and quantitative biological effect u is equal to the inverse ratio of the doses required to produce the identical effect u. The standard radiation is defined to have a specific ionization of 100 ion pairs per micron of water and this is usually taken to be conventional 200 to 300 kVp X-rays.

Summaries of the experimental results on RBE determinations for high energy electrons have been done by W. K. Sinclair and H. I. Kohn [39] and also by A. F. Holloway [40]. Including the results of previous summaries, as well as their own studies of the literature to 1963, Sinclair and Kohn found values of RBE for high energy electrons ranging from 0.61 to 1.00. Weighing these values in accordance with improved dosimetry,

they suggest that for most biological endpoints an RBE of 0.85 to 0.90 can be assigned to electrons, and interestingly also to photons, of energies from 1 MeV to 70 MeV.

However, the question was raised about the validity of assigning one value of RBE to a beam of electrons when in fact there was a spectrum of electron energies involved, and this spectrum changed with depth. Experiments had been carried out to detect a possible variation of RBE with depth, but at the time of the summary by Holloway the results were contradictory and inconclusive. An experiment by B. Markus and C. Sticinsky [41] using 14 MeV electrons on Drosophila eggs had found that at 30% and 20% dose depths, the RBEs were 19% and 22% higher than at the 100% dose depth. At the Montreux Symposium, Markus claimed to have measured an RBE of 0.61 at the 100% dose depth and 0.76 at the 30% dose depth. In contrast, H. Fritz-Niggli and H. R. Schinz [42] found no depth dependence of RBE with the 50% lethal dose on 1 hour Drosophila embryo as the biological effect. Further, a group of investigators from Villejuif presented two papers at the Montreux Symposium [43,44] which resulted in contrasting conclusions. From the first paper the survival curves of E. Coli bacteria and diploid yeast yielded an RBE for 20 MeV electrons of 0.87 with less than a 2%

variation with depth. In the second paper a clinical study on treatment of carcinoma of the tonsil compared 21 MeV electrons and 20 MeV photons, and found the electrons only 60% as effective as the photons under the most similar conditions possible. No doubt, factors other than RBE might have been involved, but this incident illustrated the difficulties and inconsistencies encountered in such studies.

The informal sessions on physics and radiobiology at the Montreux Symposium were summarized by R. Loevinger [45]. Apparently much of the discussion was centered on the question of increase of RBE with depth. Possible reasons for the discrepancies mentioned above were given and it was agreed that further systematic study be done on the question. Part of the discussion involved the role of the secondary electrons. D. Harder in opposition to R. Wideroe claimed that there was no significant change with depth in the number per rad of secondary electrons with energy less than 1 keV, but that there may be an increase in the number per rad of medium energy secondaries. The need for further physical and biological information on these questions was made clear by the discussion. In particular, what energy density in time and space is required to bring

about the change that will result in cell death or restricted reproduction?

An hypothesis on the above question and some consequences of it were presented by R. Wideroe in two papers at the Montreux Symposium [46,47]. He considers the hypothesis that inactivation of a tumor cell can only be initiated by events in which energy is concentrated in a very small volume. The mean ionization along a primary electron track produces about 6 ions per micron. Due to some clustering most of the time only 3 or 4 ions per micron are produced. On the other hand Wideroe postulates that an energy of 750 eV, sufficient to produce a cluster of 22 ions, must be deposited in less than 0.1 micron. It is suggested that such an energy concentration takes place only in the last 0.04 microns of the electron path. Thus only secondary electrons of energy greater than 750 eV, and the primary electron at the very end of its path, are capable of producing the biological effects. The choice of 750 eV as an estimate of the required energy was based on the finding that an energy of 600 to 800 eV was required to cause a double break in the strings of a DNA molecule and that similar energies are required to damage the important protein molecules of the cell. Calculations suggest that the energy lost in such concentrated events would amount

to only 6% of the total energy absorbed. Nevertheless, Wideroe's hypothesis is that such events are needed to cause primary molecular destruction.

From the primary molecular destruction to complete cell inactivation many steps are involved. Dose, dose rate, and the precise nature of the injury might determine whether a cell would recover from its injury or not. The cell itself may die, or due to damage to its DNA may not be able to produce healthy progeny. Even though many other factors are involved in inactivating the cell, the hypothesis maintains that the process must be initiated by the concentration of energy available only at the end of the track of an electron with energy greater than 750 eV.

The follow-up of the above hypothesis requires investigation by the radiation physicist on the secondary electron spectrum and its variation with depth, and by the radiobiologist on the minimum energy necessary for damaging cell components. Wideroe made some calculations on the secondary electron spectrum, and claimed that at depths where the dose began to fall off, there would be a relative increase in the number of secondary electrons of energy greater than 750 eV. Thus on the basis of his hypothesis and calculations Wideroe suggested there would be an increase in RBE with depth. As mentioned

above, Markus and Sticinsky [41] agreed with this conclusion experimentally, but it was opposed experimentally by Fritz-Niggli and Schinz [42] and theoretically by Harder.

It was in the context of such a controversy that the topic of this thesis project was suggested. A considerable amount of time has been spent in gathering, and now presenting a comprehensive report of what is involved when one talks about the energy loss of high energy electrons. Of necessity, this report in itself lacks detail, but the references cited should be adequate to provide any level of detail that one may require.

The experimental portion of this project was directed more to investigating the application of given equipment rather than an all-out attack on a given question. However, information was obtained about the variation of the energy spectrum of the secondary electrons with absorber depth.

CHAPTER III

EXPERIMENTAL EQUIPMENT, OPERATION AND CALIBRATION

Although a wide variety of experimental equipment has been employed throughout the year, only the equipment used to produce the final data will be described in this chapter. This includes the betatron, the semiconductor detector, the electronic equipment required to amplify and shape the signal from the detector, and the pulse height analyzer. The calibration of the detector and associated electronic equipment is also discussed in this chapter.

A. BETATRON

The source of the electrons was the Asklepitron 35, a 35 MeV betatron, manufactured and installed by Brown Boveri. The betatron at The Manitoba Cancer Treatment and Research Foundation is capable of producing an electron beam of continuously variable energy from 5 to 35 MeV. Output radiation could be in the form of electrons, or Bremsstrahlung produced by the electrons bombarding an internal target. Throughout the experiment, electrons were used directly.

Since the output of the betatron was in the form of 60 bursts per second, each burst 10 microseconds long,

the flux of electrons during a burst at normal operating conditions was much too high for the analysis of single events in the detector. Thus the output of the betatron had to be reduced by a factor of about 10^5 of the normal, and this output monitored by some external criteria. A common criterion was 5 to 10 counts per second from the semiconductor detector when in the standard geometry to be described later. An output matching the above criterion gave a maximum number of events to analyze without any significant number of coincident events.

The adjustments required to produce the desired output from the betatron will be described in Appendix B. Comments on general procedures that might be followed in other applications will be included.

As the betatron was used daily for treatment, the experiment had to be run discontinuously. In order to reproduce the geometry reliably the betatron was set horizontal and the treatment bed moved so that its pivotal axis was along the central axis of the electron beam and one meter from the end of the beam defining cone. The bed was turned 7° to set it perpendicular to the direction of the beam. A cardboard template was fixed to the treatment bed and positions could then be referred to a co-ordinate system on the cardboard with the pivotal axis of the bed as the origin. The standard geometry was with the detector

placed at this origin.

The electron beam shape was defined by a 4 cm circular cone. A film cross section of this beam at 1 m from the cone showed that the 50% isodose curve was about 5 cm in diameter. Since the detectors were less than 1 cm in diameter an error of up to 1 cm in positioning still left the detector effectively in the center of the beam.

B. SEMICONDUCTOR DETECTORS

A semiconductor detector is in essence a solid ionization chamber. Instead of dealing with the production and collection of electron and positive ion pairs, one considers electron-hole pairs in a semiconducting medium. By applying a reverse bias across a p-n junction of high purity silicon or germanium a high resistance sensitive volume, or depletion zone is formed. In this depletion zone the number of free charged carriers is reduced and thus there is a minimum background of thermal noise. When an ionizing particle traverses the sensitive region, electron-hole pairs are created. Due to the applied electric field, these are collected within nanoseconds, producing a small, short, current pulse in the external circuit. Since the energy required to produce an electron-hole pair is constant for ionizing radiation with a wide range of

energies and ionization densities, the detector response is a linear measure of the energy deposited in its sensitive volume. Further, the energy loss per electron-hole pair is only 3.6 eV for silicon, and less for germanium, as compared to about 35 eV per ion pair in an air ion chamber. Thus for a given energy loss, ten times as many free charge carriers are produced in the semiconductor detector, giving it an inherently superior resolution to other detector systems. The higher stopping power of the solid, the fast recovery time due to high carrier mobility and small detector volume, and the long-term stability of a solid state device are also desirable features of a semiconductor detector.

At present the depletion depths available are limited to a few millimeters for lithium-drifted detectors and to one millimeter for junction detectors. Thus only heavy ions of high energy can be totally stopped in such a detector. Light particles, such as electrons, of high energy pass directly through and one measures only the energy loss per depletion depth. In such cases it is advantageous to have a detector that is fully depleted so the total volume is sensitive to the ionizing particle and the detector thickness defines the depth over which the energy is deposited. Such a detector is usually in a transmission mount allowing a beam of high energy particles to pass through relatively undisturbed, available for further

study if desired.

There are some features of a semiconductor detector that require special notice for satisfactory operation. Most semiconductor detectors are sensitive to light unless their surfaces have been specially painted. Also, operating temperature imposes some restrictions on the performance of a semiconductor. All germanium detectors must be cooled to liquid nitrogen temperature, but silicon detectors can be operated satisfactorily at room temperature.

Two fully depleted silicon junction detectors were used in the course of the experiment. The first was a surface barrier detector in a transmission mount and was supplied by ORTEC. A diagram and the specifications of this detector are shown in Figure 2. To protect the sensitive faces and shield it from light, this detector was mounted in a brass tube, 3.5 cm in diameter and 5 cm long, with the ends capped by a thin mylar-aluminum foil. The second was a multi-diffused junction detector supplied by Molechem Inc. This detector had a more rugged surface than the surface barrier detector and thus was mounted with front surface exposed in a water-tight enclosure. The detector is shown with its specifications in Figure 3. A piece of the mylar-aluminum foil glued to the rim of the detector mount provided light shielding. Although these detectors utilize different means for obtaining a junction, have opposite

FIGURE 2

ORTEC DETECTOR

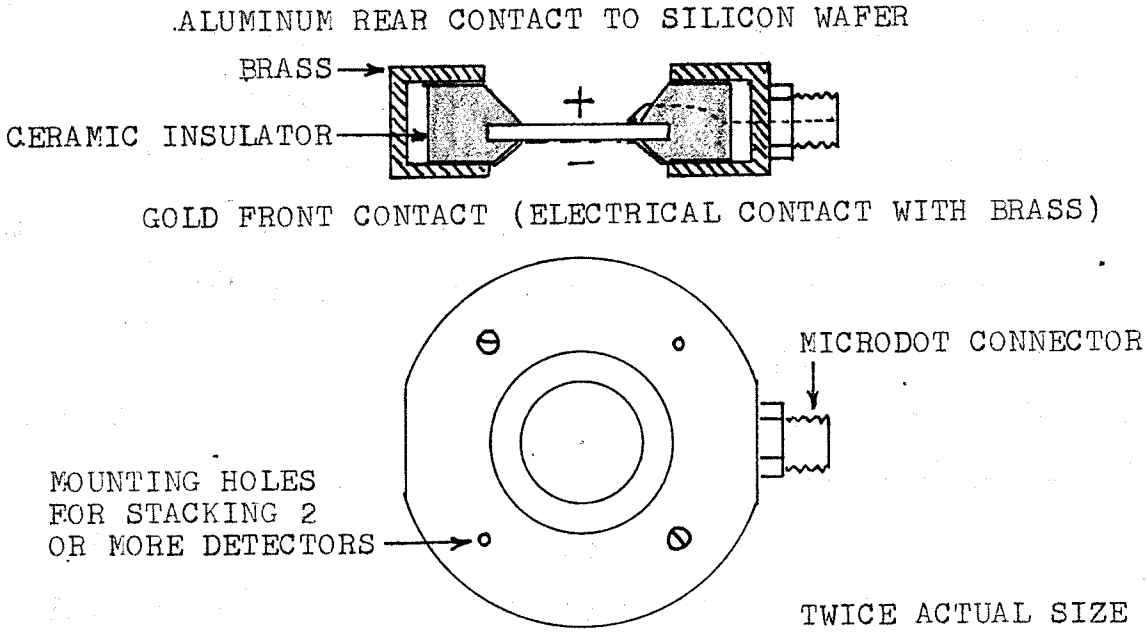

SPECIFICATIONS

TYPE:	Silicon, fully depleted, surface barrier detector in transmission mount
SERIAL NUMBER:	5-358A
ACTIVE AREA:	50 mm^2
THICKNESS:	450 microns
BIAS VOLTAGE:	+80 Volts for total depletion
REVERSE CURRENT:	0.18 microAmperes
NOISE WIDTH:	12 keV

FIGURE 3

MOLECHEM DETECTOR

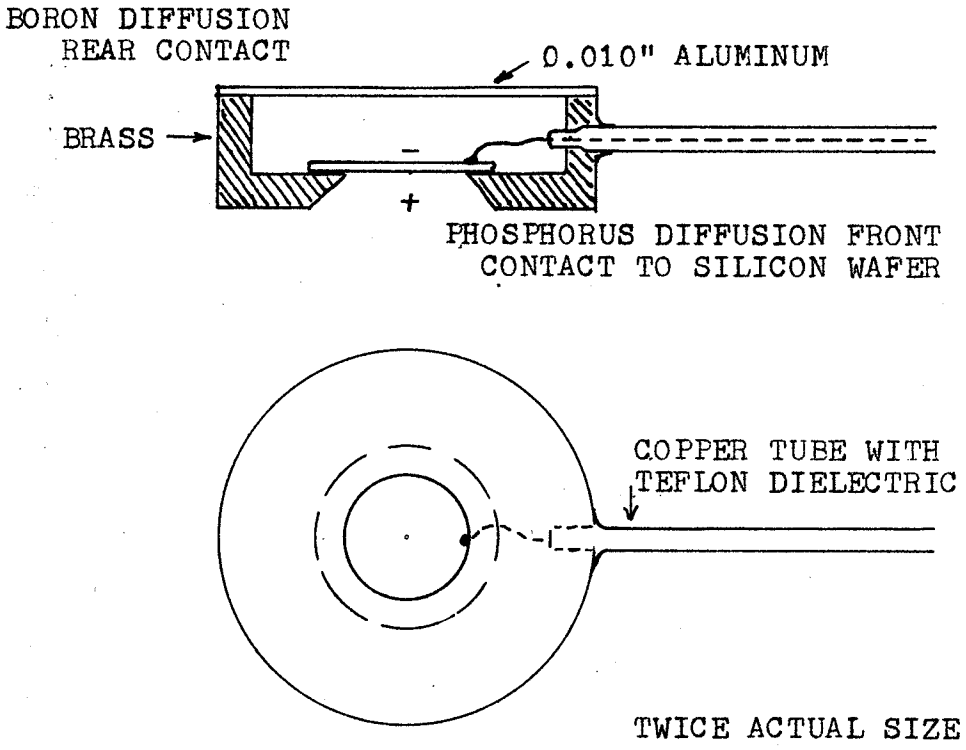

SPECIFICATIONS

TYPE:	Silicon, fully depleted, multi-diffused junction detector in a special watertight enclosure
ACTIVE AREA:	50 mm^2
THICKNESS:	220 microns
BIAS VOLTAGE:	-200 volts for total depletion
REVERSE CURRENT:	2 microAmperes
NOISE WIDTH:	15 keV

biasing polarities, and are mounted differently, their response to radiation is identical and after calibration the results from each may be compared very closely apart from the differences due to thickness.

C. ELECTRONIC EQUIPMENT

In order to make best use of the speed, the high resolution, and the linear output of a semiconductor detector, high performance electronic equipment is required. Of utmost importance is the preamplifier. It must convert the small current pulse from the detector to a substantial output voltage pulse which can be driven through a long connecting cable to a voltage and pulse shaping main amplifier. The ORTEC Model 109 all transistor preamplifier was used. It utilizes a field-effect transistor as the input stage of a charge sensitive input loop. If the input capacity is kept low, that is less than 100 picofarads, this input stage introduces very little noise and the output is completely independent of the detector bias voltage. To minimize the input capacitance, the preamplifier was placed near the detector with a special two foot, low capacitance cable connecting them.

By isolating the bias supply from the input circuit with a capacitor the detector bias was applied along the same

cable. A load resistor of 100 megohms was included in series with the bias supply. The voltage drop across this resistor as a result of the detector leakage current had to be taken into account when determining the applied detector bias.

Through a special connector, a test pulse could be applied independently to the input of the preamplifier. This allowed a check on the operation of the electronic equipment, and also routine calibration of the system. A Sharp Model PRG-159, Precision Pulse Generator was used as the test source.

No pulse shaping was done in the preamplifier, apart from a 50 microsecond decay constant so the signal would return to zero in a reasonable time. Thus the output signals had a sharp rise time of less than 100 nanoseconds and the imposed decay time of 50 microseconds. To prepare these signals for the external input of the pulse height analyzer (PHA) a pulse shaping voltage amplifier was required. For this function Nuclear Enterprises Ltd., Model NE 5230, General Purpose Pulse Amplifier was used. By choosing equal differentiation and integration time constants of 0.5 microseconds this amplifier improved the signal to noise ratio about three times for the range of signals used. Almost all of the low frequency noise that was generated in the detector, and appeared in the preamplifier, was eliminated by the low frequency cut-off characteristics of the amplifier. The

resulting output pulse had a nearly symmetric rise and fall and a total width of about 2 microseconds, forming an ideal input for the PHA.

Pulse height analysis was done using a four hundred channel analyzer, Model 20631, supplied by Radiation Counter Laboratories, Inc. Four groups of one hundred channels each could be used separately. Instantaneous display of the spectrum of number of counts versus channel number was available on an oscilloscope. A few of the final spectra were recorded photographically by means of an oscilloscope camera with Polaroid film pack. Printout facilities, which listed the number of counts in each channel were used whenever data was required for permanent reference or for further numerical analysis.

Physically the above system was arranged with the detector and preamplifier on the treatment bed; the preamplifier power supply, detector bias, and main amplifier on a separate stand in the betatron room; and the PHA near the betatron control console outside the treatment room. The input to the PHA was routinely monitored with an oscilloscope to allow instantaneous check on the operation of the equipment and to give a qualitative measure of the betatron output. A block diagram of the equipment is given in Figure 4, and Figure 5 is a picture of the equipment as arranged around the betatron.

FIGURE 4

BLOCK DIAGRAM OF ELECTRONIC EQUIPMENT

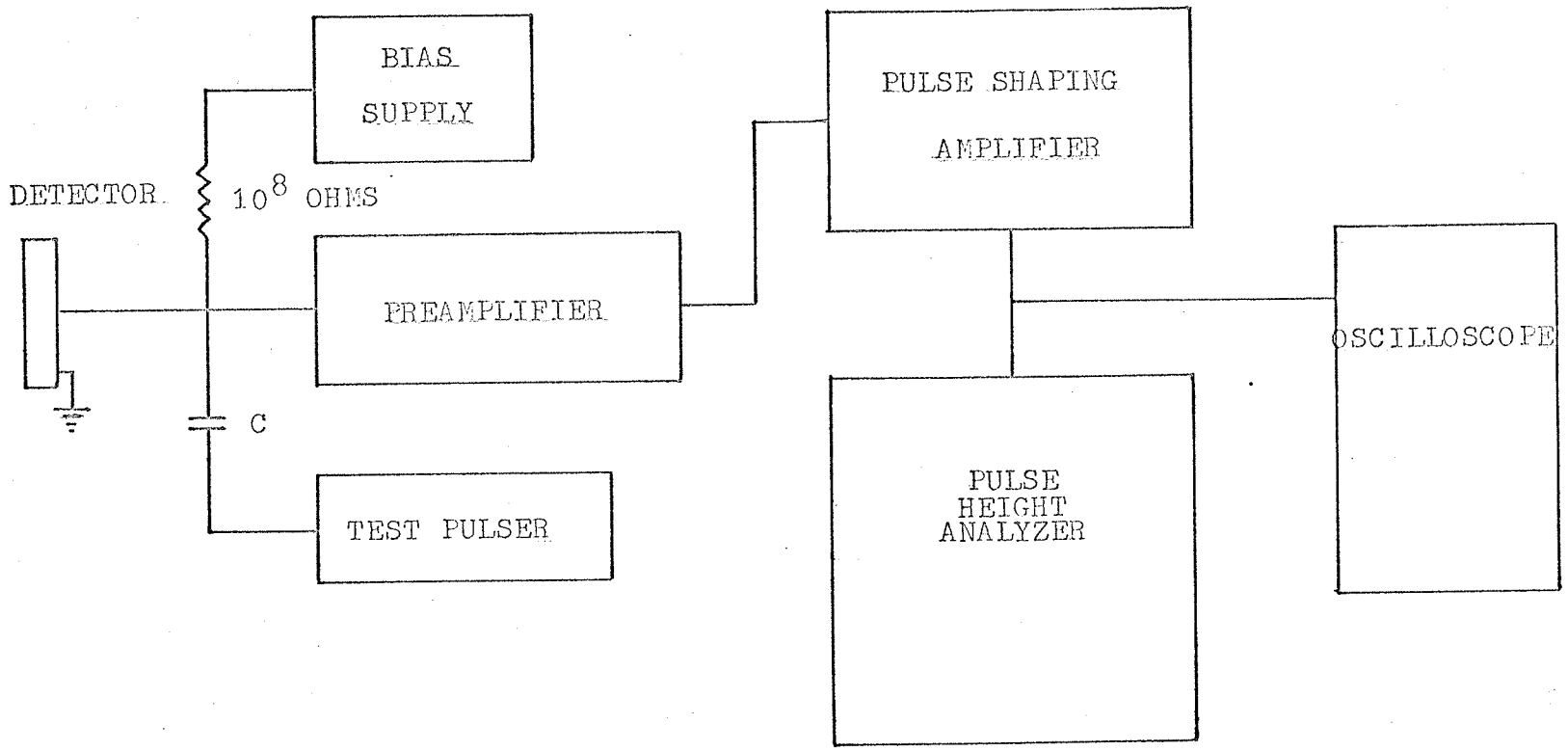

FIGURE 5

DETECTOR AND ELECTRONIC EQUIPMENT

AROUND THE BETATRON

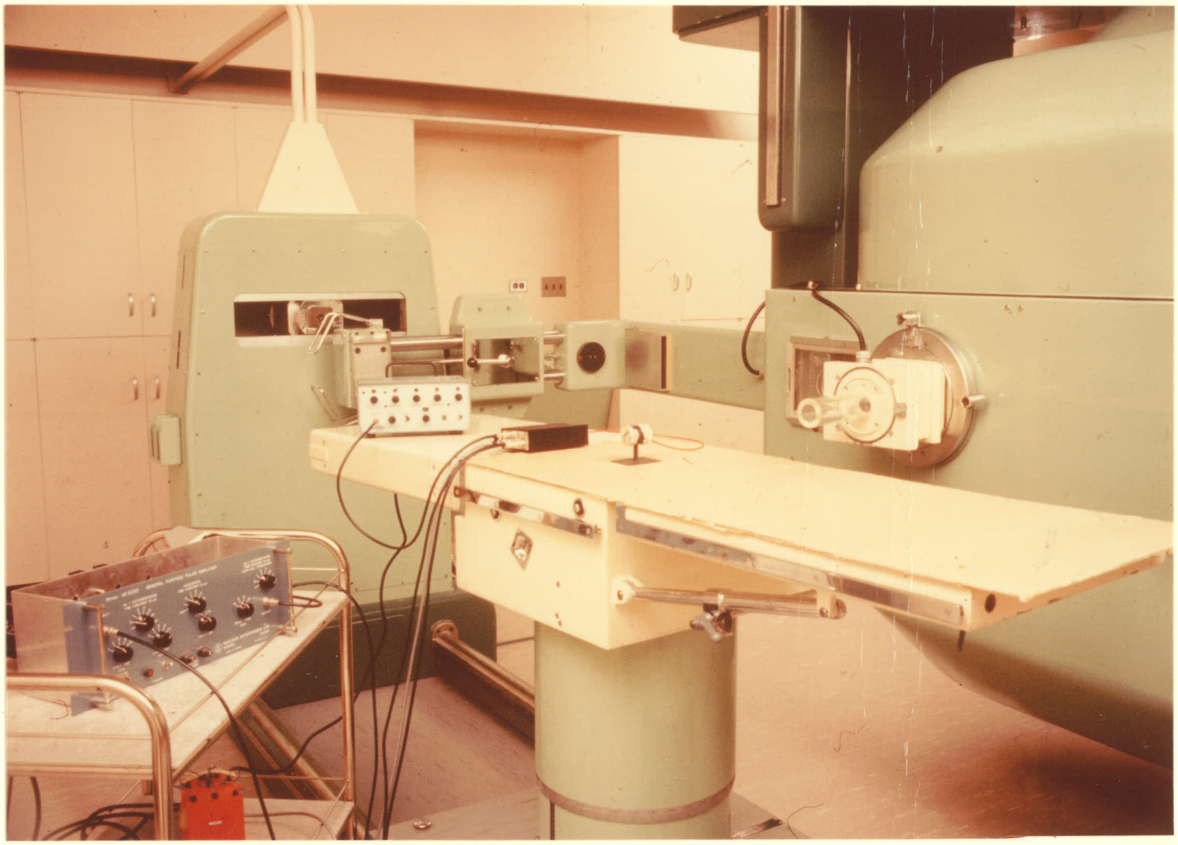

D. CALIBRATION

Calibration of the detector, amplifier and pulse analysis system required two steps. The test pulses were calibrated in terms of a known energy deposit in the detector, and then the pulse generator could be used to extend the calibration over a wider range and to allow routine checks on the calibration. Key to the validity of such an approach is the fact that the pulse generator produces pulses similar to those produced by the detector, and these are applied at the input of the preamplifier.

Absolute energy calibration of the detector and pulse analysis system was accomplished by means of a Bi^{207} source. This source was mounted with an open surface so that the K and L internal conversion electrons of two decay gamma rays could be observed. The gamma rays had energies of 0.570 MeV and 1.064 MeV resulting in internal conversion electrons of 482 keV, 554 keV, 976 keV and 1.049 MeV. Although these energies were higher than the rated stopping powers of the detectors, due to multiple scattering, a sufficient number of the electrons were completely stopped so that peaks corresponding to the above energies were produced. Those electrons which were not completely stopped contributed to the broad minimum ionization peak with energy

dependent on the detector thickness.

By a graphical method all four electron energies were used to calculate the ratio of energy deposition in the detector to test pulse voltage. When applied to the curves of test pulse voltage versus channel number made at the normal data collection operating ranges, this conversion factor gave the curve of energy versus channel number.

The conversion factor was 22.5 keV per millivolt for the ORTEC detector and 22.9 keV per millivolt for the Molechem detector. Figures 6 and 7 are the respective calibration curves of these two detectors. During data collection two points on these curves were regularly checked.

Resolution of the pulse height analysis system was determined by measuring the full width at half-maximum of a peak due to test pulses. The results suggested a resolution of about 12 keV for the ORTEC detector and about 15 keV for the Molechem detector. These values include the broadening due to noise that will affect all distribution to be analyzed.

Calibration of the energy of the betatron beam has been carried out recently by J. Ramnath [48], by means of threshold reactions in the region of 10 MeV to 30 MeV. On the basis of his results, and extrapolating linearly,

FIGURE 6

CALIBRATION CURVE FOR ORTEC DETECTOR

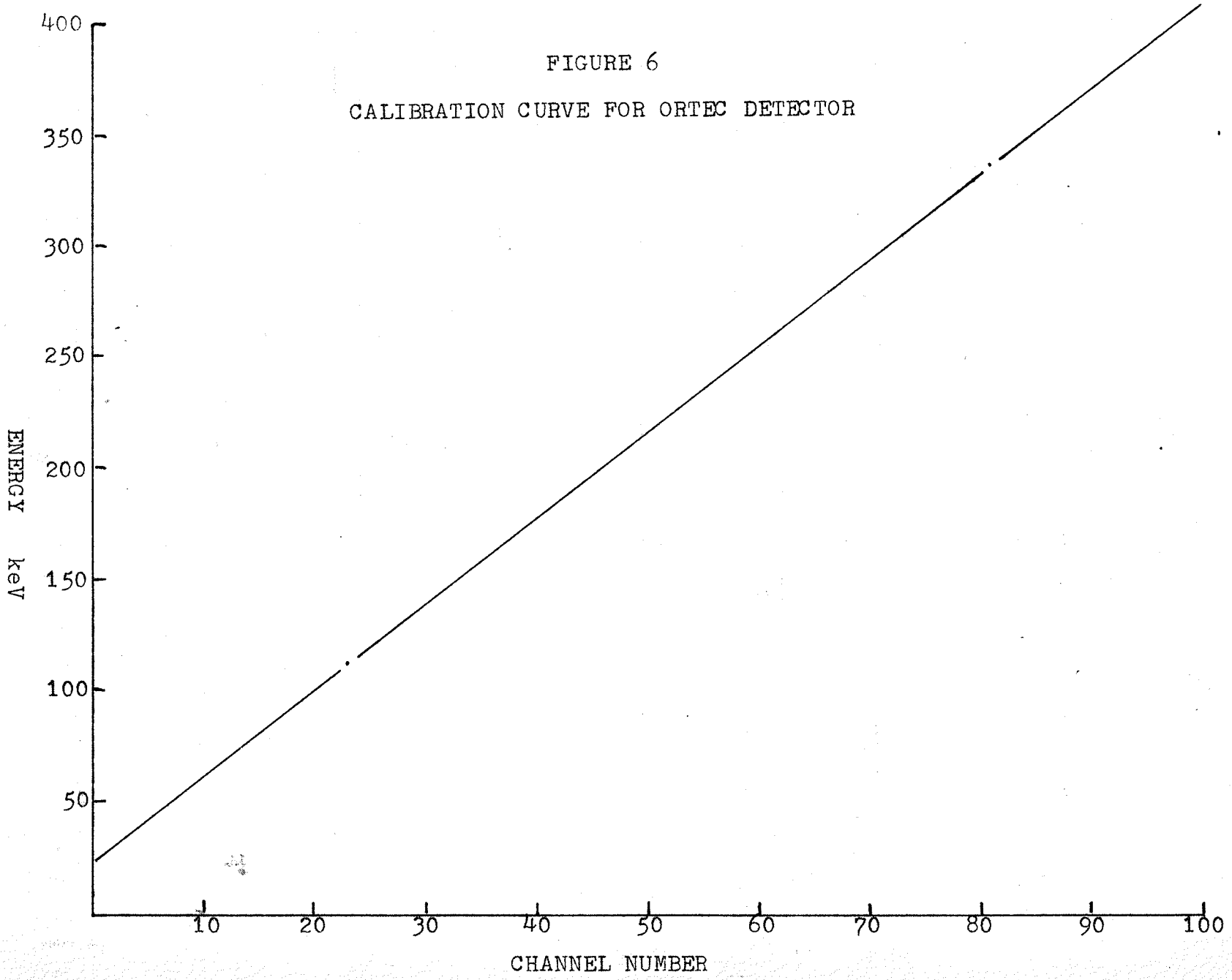

FIGURE 7

CALIBRATION CURVE FOR MOLECHEM DETECTOR

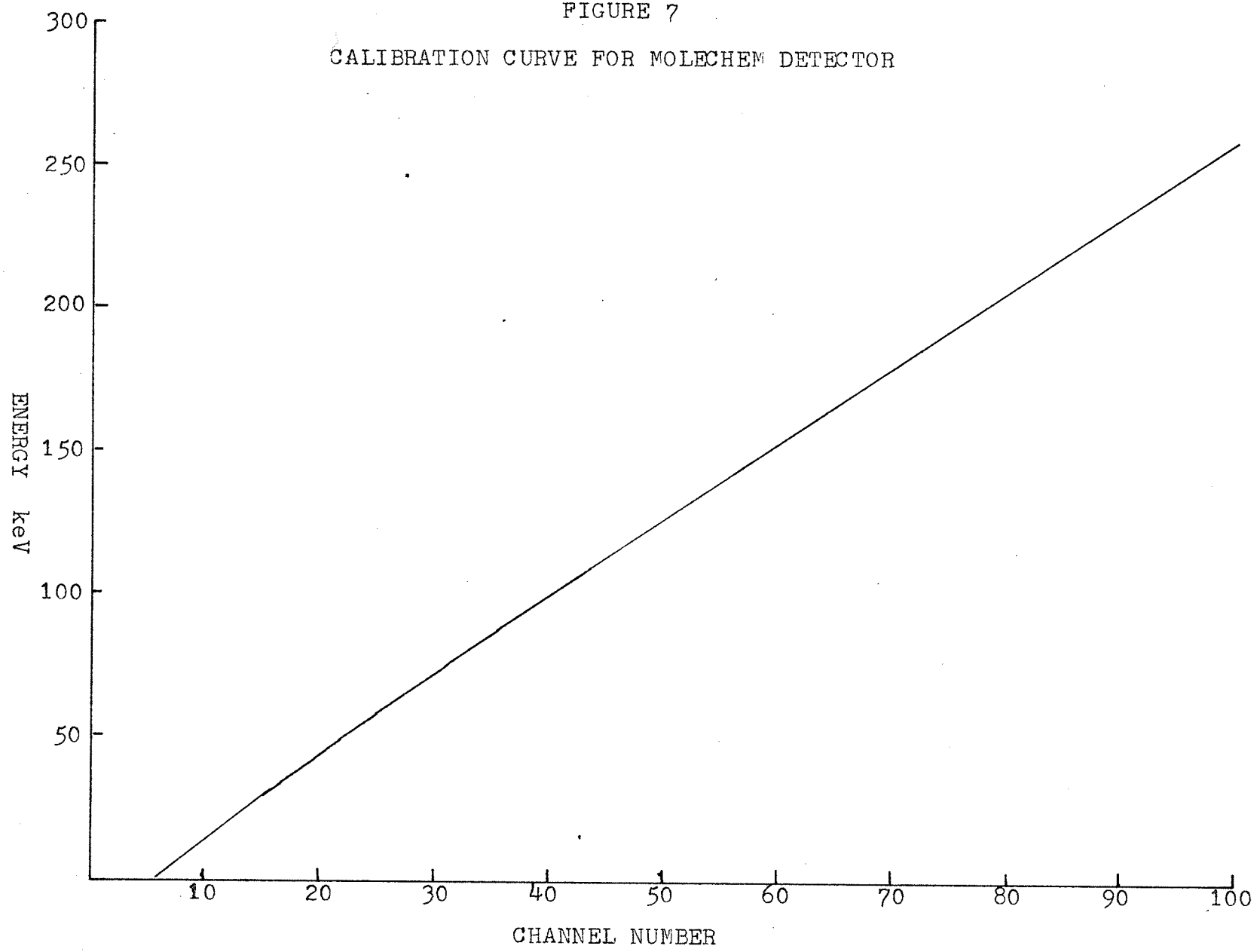

the dial settings of 20 MeV and 35 MeV that were used in the experiment, correspond to 20.2 MeV and 34.8 MeV at the end of the field defining cone.

Some energy was lost in the beam monitoring transmission chamber. Since the detector was normally one meter from the cone face, further energy was lost to the air. However, the experimental results were only slowly dependent on energy, and the electron beam was accepted as having a nominal energy of 20 MeV and 35 MeV when used in the experiment.

CHAPTER IV

DATA COLLECTION AND NUMERICAL ANALYSIS

Under the operating conditions described in the last chapter, the detector system yielded the spectrum of energy deposits due to individual electrons as they were stopped inside, or passed through the detector material. With lucite placed in front of the detector, the variations in the spectrum due to increasing depth in an absorbing material were recorded. The procedures used in obtaining this data, normalizing it, and then calculating appropriate parameters of the spectra are described in this chapter.

Electrons with energies of 35 MeV and 20 MeV were used in the experiment. Trials were run at each of these energies from zero depth in lucite up to a depth sufficient to reduce the relative depth dose to less than 10%. In this connection an "effective density" of 1.11 gms per cm^3 was assigned to lucite. This was suggested by R. Loevinger et al [49] in order to be able to scale the depth dose curves for water to depth dose curves for lucite. Thus the relative dose corresponding to a given depth of lucite could be determined.

Each trial was run for fifteen minutes, in which time 2,000 to 8,000 counts were accumulated over the entire spectrum. The total number of counts in each trial did not

follow any systematic pattern, as the betatron output was adjusted for each trial and would also drift to some extent during a trial.

A series of spectra obtained from the ORTEC detector was photographed and is shown in Figure 8. These spectra were for 20 MeV electrons penetrating from 0 cm to 7.8 cm of lucite. It is to be emphasized that these spectra do not represent the energy of the electrons, nor the amount of energy delivered to a given depth in lucite. Rather, they show the spectrum of energies deposited in the volume of the detector by individual electrons at a given depth in lucite. The spectra from the ORTEC detector for 35 MeV electrons at depths of 0 to 14 cm lucite were remarkably similar to those shown in Figure 8. Spectra of similar shape were also obtained from the Molechem detector, although the peaks corresponded to a much lower energy deposition and the level of electronic noise was considerably higher. With the ORTEC detector, electronic noise corresponding to an energy of 35 keV occurred and filled the channels up to the fifth, while with the Molechem detector the noise level was up to 40 keV and filled the channels up to the seventeenth.

Thus, out of necessity, analysis of the data from the Molechem detector could not proceed below channel 18. Analysis of the peak of the spectrum was

FIGURE 8

ENERGY DISSIPATION SPECTRA OF 20 MEV ELECTRONS
IN THE ORTEC DETECTOR
AT INCREASING DEPTHS OF LUCITE

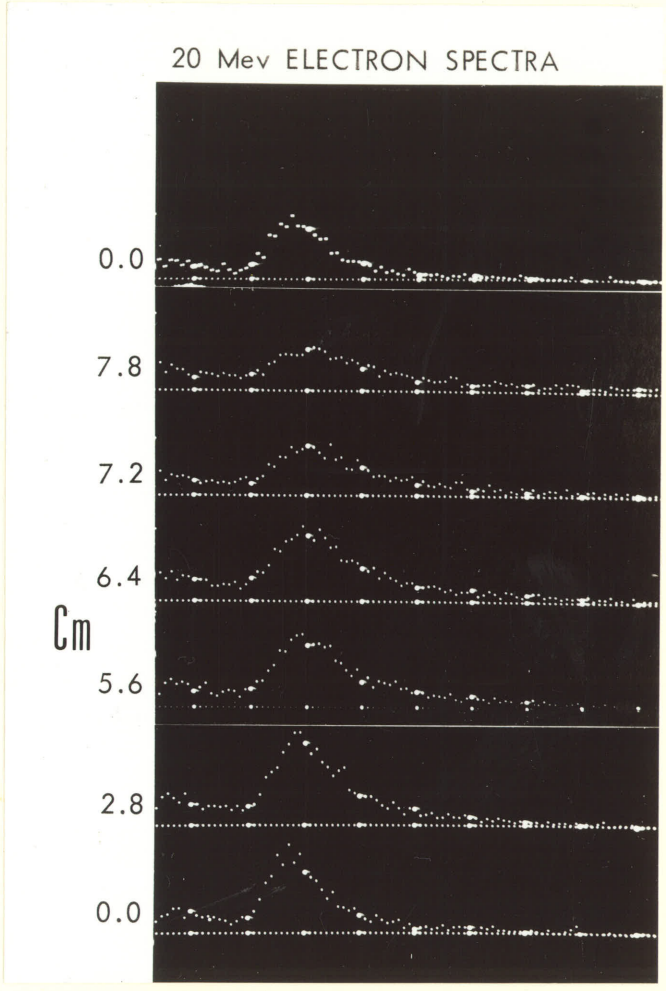

THE ORDINATE FOR EACH TRACE IS NUMBER OF COUNTS AT THE GIVEN DEPTH

allowed, but no information at energies lower than the peak was available.

As shown in Figure 8, the spectra from the ORTEC detector included a definite low energy tail below the peak. The source of this low energy tail was not immediately evident. It is unlikely that much of this tail was due to primary electrons themselves. There was some evidence that part of the low energy tail was the result of γ-rays, X-rays, or Compton electrons, as well as secondary electrons from the primaries. Tests that might have given the answer were considered, but before they could be carried out the ORTEC detector broke down and could not be replaced in time for new information to be included in this thesis. It was decided that the spectra of the ORTEC detector would be analyzed only above channel 20, so as to include the peak and the high energy tail. Thus the study was limited to the primary electrons themselves or to other events that deposited as much energy as a primary electron. Also, by choosing the low energy base of the peak as the cut-off point for the analysis of the spectra from the ORTEC detector, the span of analysis was made to coincide with that available on the spectra from the Molechem detector. For the ORTEC detector, the range of study was from channel 20 to 99, which corresponded to energy deposits of 100 keV to 410 keV; for the Molechem

detector the range was from channel 18 to 99, i.e. energy deposits of 40 keV to 260 keV.

As mentioned earlier, there were considerable variations from trial to trial in the total number of counts contained within each spectrum. To permit direct comparison between trials all spectra were normalized to a total of ten thousand counts over the appropriate range of analysis. These normalized spectra were plotted, and the energy of the peaks determined. The mean energy of each spectrum was also calculated.

CHAPTER V

EXPERIMENTAL RESULTS AND THEORETICAL CALCULATIONS

With the data processed as described in the last chapter, the experimental results were arranged so as to allow comparisons from trial to trial. Theoretical calculations were made for comparison with the experimental parameters. A description of the results and a discussion of the implications thereof are included in this chapter.

A. EXPERIMENTAL RESULTS

Series of normalized spectra from the two detectors are given in Figures 9 and 10. Figure 9 is for 20 MeV electrons incident on the ORTEC detector through increasing thickness of lucite. The spectra for 35 MeV electrons incident on the ORTEC detector are not shown, but they were qualitatively identical to those for 20 MeV electrons. For the Molechem detector the spectra for 35 MeV electrons are shown in Figure 10. Very similar results were obtained for 20 MeV electrons, but these are not shown. A list of the energies of the peaks and of the mean energies for all the spectra that were analyzed is given in Table I.

B. THEORETICAL CALCULATIONS

It was necessary to compare the experimental results with theoretical calculations, before the true significance

FIGURE 9

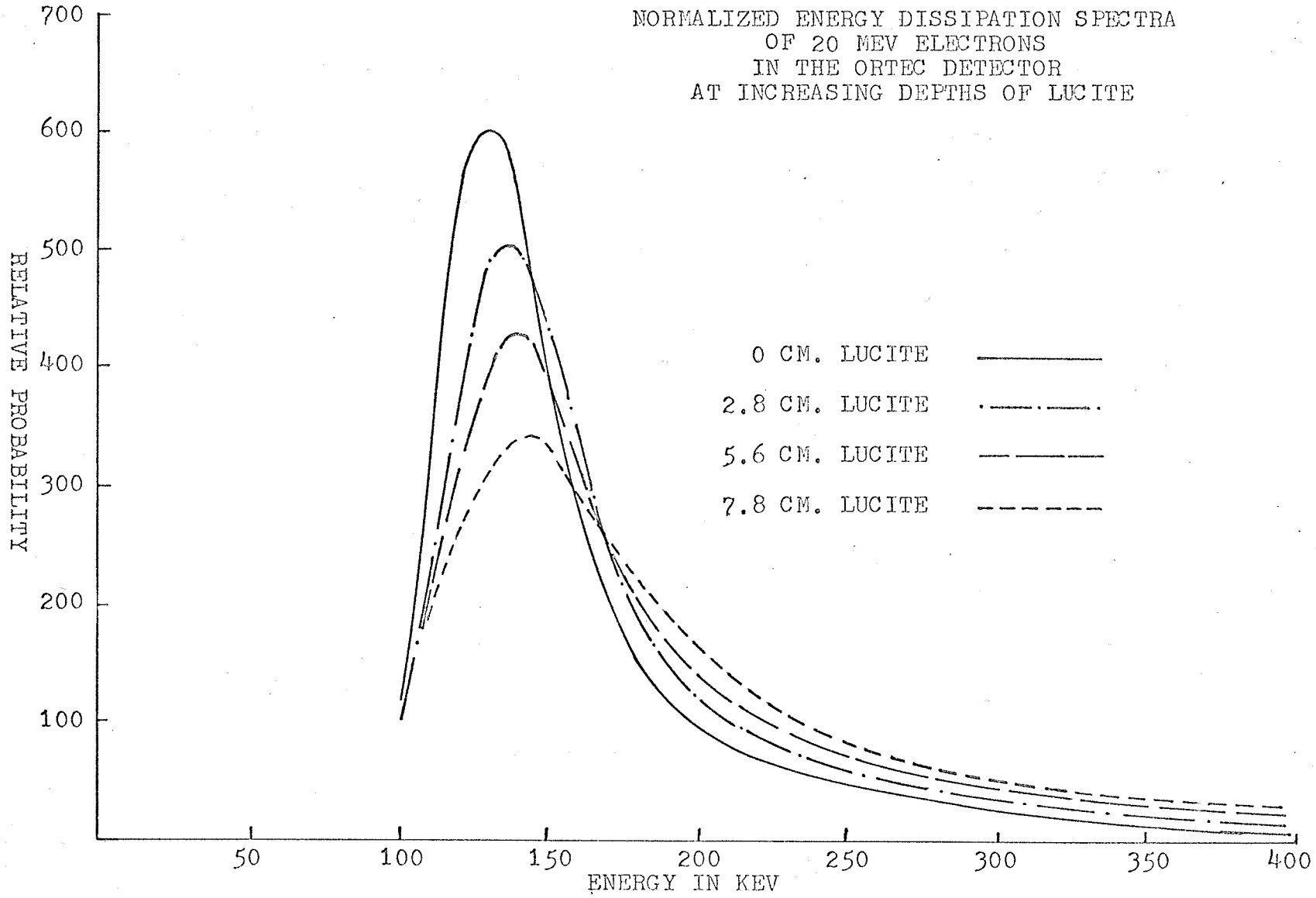
NORMALIZED ENERGY DISSIPATION SPECTRA
OF 20 MEV ELECTRONS
IN THE ORTEC DETECTOR
AT INCREASING DEPTHS OF LUCITE
0 CM. LUCITE
2.8 CM. LUCITE
5.6 CM. LUCITE
7.8 CM. LUCITE
RELATIVE PROBABILITY
700
600
500
400
300
200
100
50
100
150
200
250
300
350
400
ENERGY IN KEV

FIGURE 10

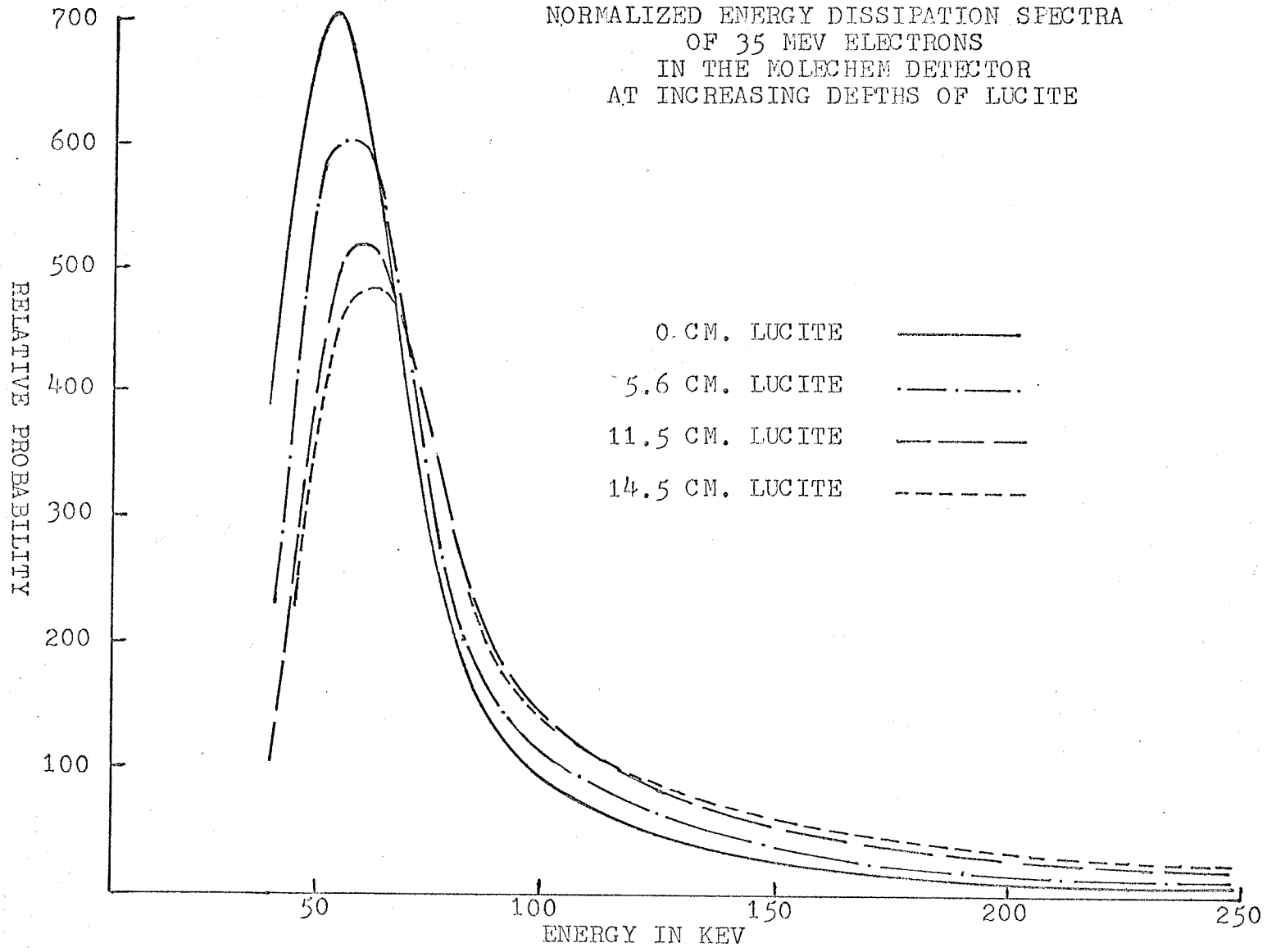
NORMALIZED ENERGY DISSIPATION SPECTRA
OF 35 MEV ELECTRONS
IN THE MOLECHEM DETECTOR
AT INCREASING DEPTHS OF LUCITE
0 CM. LUCITE
5.6 CM. LUCITE
11.5 CM. LUCITE
14.5 CM. LUCITE
RELATIVE PROBABILITY
700
600
500
400
300
200
100
50
100
150
200
250
ENERGY IN KEV

TABLE I

ENERGIES OF THE PEAKS AND OF THE MEANS

OF THE EXPERIMENTAL SPECTRA

	DEPTH IN LUCITE (cm.)	MOST PROBABLE ENERGY LOSS (keV)	MEAN ENERGY (keV)
ORTEC DETECTOR:			
20 MeV	0	128	162
	2.8	133	174
	5.6	135	183
	6.4	138	184
	7.2	141	190
	7.8	140	196
35 MeV	0	128	164
	5.6	135	171
	11.2	138	178
	13.0	136	184
	14.0	137	189
MOLECHEM DETECTOR:			
20 MeV	0	58	75
	2.8	61	83
	4.8	64	94
	6.4	61	92
	7.4	61	96
	8.4	61	98
	9.2	61	99
35 MeV	0	56	74
	5.6	58	82
	11.5	60	92
	13.2	64	94
	14.6	60	94
	16.3	61	94
	25.0	60	95

of the spectra was apparent. To begin with, only the spectra that were accumulated without any absorber in front of the detector were compared with the calculations.

The mean mass stopping power for Si was determined from equation (A-2) of Appendix A. If the stopping of an electron were a completely continuous process, an "expected mean energy loss" could be calculated by multiplying the mass stopping power by the density of Si and by the thickness of the appropriate detector. This was done for both detectors for energies from 1.5 MeV to 35 MeV and the results are listed in Table II.

The stopping of an electron, however, is not continuous. Included in the mean rate of energy loss of an electron are a few extremely large energy transfers to high energy secondary electrons. In a thin slab of material the probability is very small that such a large energy transfer will occur. Thus in the thin Si detectors energy losses considerably lower than the "expected mean energy loss" were more likely to be observed. In fact, the peak of the spectrum was the most probable energy loss in the detector. The skewed shape of all the spectra verified that the most probable energy loss was lower than the mean energy loss. The most probable energy loss was calculated with the aid of two parameters that are defined below. The derivation

TABLE II

THEORETICAL CALCULATIONS

FOR ORTEC DETECTOR:

Energy of electron in MeV	35	20	10	5	1.5
"Expected mean energy loss" in keV	193	186	179	171	160
W_1 in keV	8.0	8.0	8.0	8.0	8.5
$g_1 = \frac{W1}{E}$ $(x10^{-4})$	2.3	4.0	8.0	16.0	53.0
P_1	0.66	0.68	0.70	0.71	0.75
Most probable energy loss in keV	127	127	126	121	120
$g_2 = \frac{.5}{E}$ $(x10^{-2})$	1.4	2.5	5	10	33
P_2	0.85	0.87	0.89	0.93	0.98
Mean energy loss in keV	163	162	159	157	157

FOR MOLECHEM DETECTOR:

Energy of electron in MeV	35	20	10	5	1.5
"Expected mean energy loss" in keV	94	91	88	84	78
W_1 in keV	4	4	4	4	4.3
$g_1 = \frac{W1}{E}$ $(x10^{-4})$	1.1	2.0	4.0	8.0	29
P_1	0.63	0.65	0.66	0.68	0.71
Most probable energy loss in keV	59	59	58	57	56
$g_2 = \frac{.25}{E}$ $(x10^{-3})$	7.1	12.5	25	50	160
P_2	0.81	0.84	0.87	0.90	0.95
Mean energy loss in keV	76	76	76	75	74

of these parameters and the means for calculating them are included in Appendix A.

One may calculate a restricted stopping power which does not include the energy lost from the electron due to individual transfers of energy above a maximum allowed value. For a given primary electron of energy E, the restriction, or maximum allowed value of secondary electron energy to be included in determining the stopping of the electron, can be any fraction g, up to one-half of the primary energy. Then the restricted stopping power for an electron of energy E, as a function of the fraction g, is best represented as the ratio of the restricted stopping power to the unrestricted stopping power. If this ratio is represented by P, then the graph of P versus log g for a given energy E is a straight line. This graph for a series of values of E is given in Figure A-1, of Appendix A.

The second parameter is related to the probability for a given transfer of energy to occur, or equivalently, for a secondary electron of given energy to be produced. The parameter W_1 is that individual transfer of energy which will on the average take place just once as the primary traverses the distance X of the stopping media. For Si, the value of W_1 is given by equation (A-4) of Appendix A. With the distance X set equal to the thickness in cm of the appropriate detector, W_1 is the maximum individual

energy transfer in keV that is likely to occur as the electron passes through the detector. In essence, for most electrons, W_1 is the maximum single collisional energy loss allowed in the detector. Thus for a beam of electrons of energy E, the most probable rate of energy loss should be given by the restricted stopping power appropriate to the restriction W_1. To calculate the restricted stopping power, Figure A-1 was used to determine P for the energy E where the fraction g was given by $\frac{W_1}{E}$. Then P times the mass stopping power was the restricted mass stopping power. The most probable energy loss was given by P times the "expected mean energy loss". These values are included in Table II. Of course, larger losses could occur, and thus the mean energy loss was greater than the most probable energy loss.

However, the mean energy losses determined from the experimental spectra were still considerably lower than the "expected mean energy losses". This was explained by the fact that some of the energy lost by the electron while in the detector was carried out of the detector by high energy secondaries. Thus, although such an interaction would contribute to the expression for the "expected mean energy loss" it would not register as an energy loss in the detector. A 380 keV electron has a range equivalent to the thickness of the ORTEC detector. Correspondingly

the Molechem detector could stop only a 230 keV electron directed straight at it. Thus, some of the high energy secondary electrons would readily pass out of the detector. Since the secondaries would be generated at an angle to the small dimension of the detector, and at all depths, it was estimated that on the average a secondary of greater than 500 keV would escape from the ORTEC detector. For the Molechem detector a secondary with 250 keV would likely escape. Thus discrete energy losses greater than the above values in effect were not noticed by the detector and the mean energy loss in the detector was lower than the "expected mean energy loss". The mean energy loss was calculated from P times the "expected mean energy loss" where P was evaluated at $g = \frac{500 \text{ keV}}{E}$ and $g = \frac{250 \text{ keV}}{E}$ for the appropriate detector. These results are found in Table II.

C. COMPARISON OF RESULTS WHEN NO ABSORBER IS INVOLVED

The theoretical calculations for the most probable energy loss and the mean energy loss at both 20 MeV and 35 MeV agreed well with the experimental results from the ORTEC detector with no absorber in front of it. The spread of energy within each channel was approximately 4 keV, and the results coincided well within this limit, which is a variation of less than 3%.

For the Molechem detector with no absorber the

experimental values of the parameters were all 1 to 3 keV lower than the calculated values. The spread per channel for this detector was 2.5 keV so that the discrepancy amounted to about one channel. This represented a difference of about 5%. A systematic error in the order of 2 keV may have been introduced in the calibration, or the detector may have been slightly thinner than rated.

Since the spectra in Figures 9 and 10 were plotted against channel number and the two detectors had different calibration curves, the comparison between detectors could not be made directly. Figure 11 shows the results from the two detectors plotted on the same energy scale. The results were for 20 MeV electrons with no absorber. It was noted that the shapes were similar but the ORTEC detector produced a broader spectrum. This was in line with the comment made by Bethe and Ashkin [3], that the full width at half maximum for the most probable energy distribution would be slightly greater than four times the value of W_1. When the broadening due to electronic noise was subtracted, the FWHM was 15 keV for the Molechem detector and 37 keV for the ORTEC detector. The values of W_1, as previously calculated, were 4 keV and 8 keV respectively, and so the peaks have a width in the order of what would be expected.

D. COMPARISON OF RESULTS AT INCREASING DEPTHS OF ABSORBER

With the shape of the spectra explained, and

FIGURE 11

COMPARISON OF RESOLUTION
OF ORTEC AND MOLECHEM DETECTORS

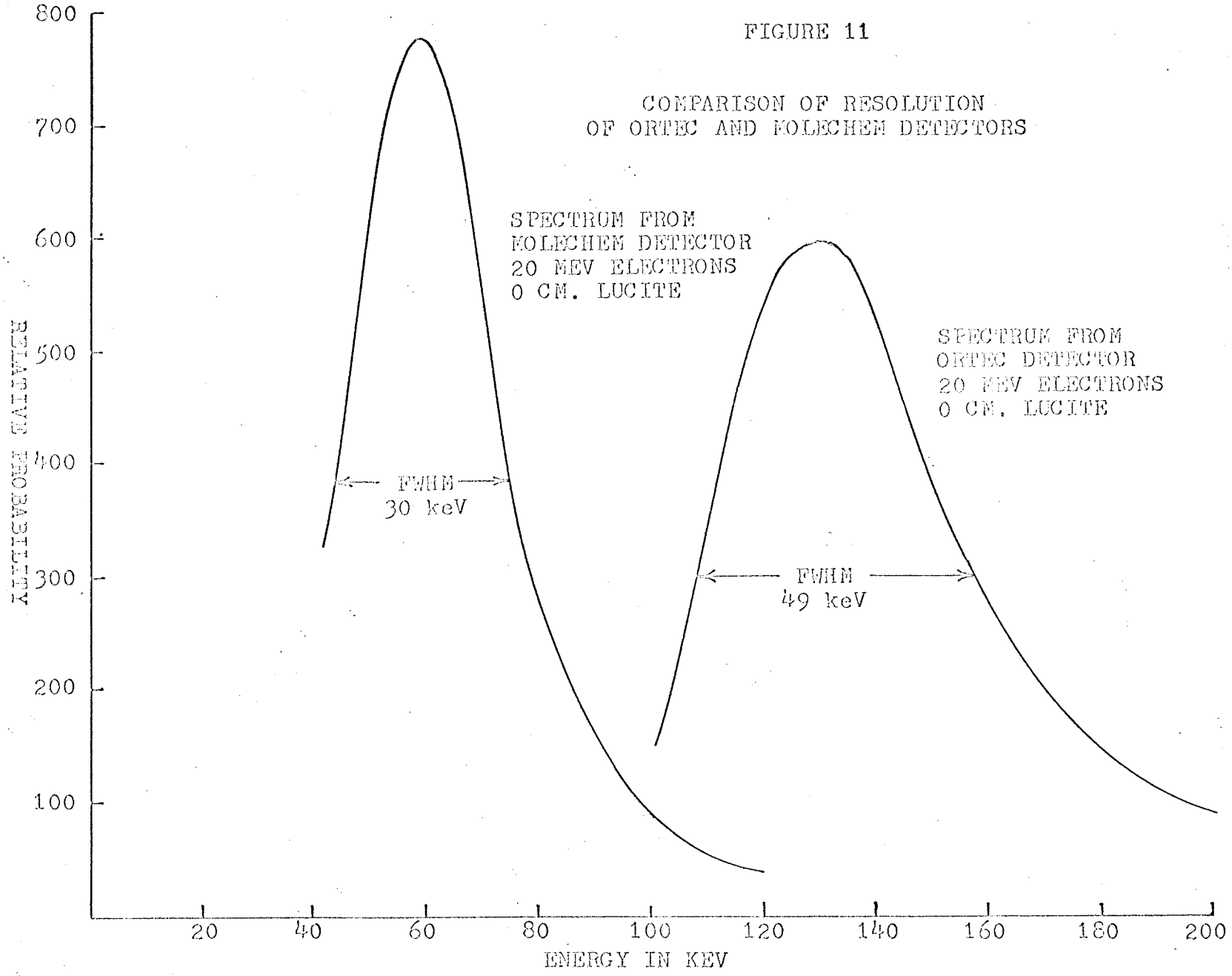

experimental values of the parameters in good agreement with the calculations, it was then possible to consider the variations from trial to trial. The trends are clearly shown in Figures 9 and 10. With increasing depths in the lucite the peak of the spectrum shifted to slightly higher energy and broadened considerably. There was a decrease in peak height with a corresponding increase in the number of higher energy deposits at greater depths. The mean energy loss increased with depth more rapidly than the most probable energy loss.

Once depths corresponding to a depth dose of less than 10% were attained the spectra assumed a stationary shape that did not change with further increase in depth. This was apparent in particular for 35 MeV electrons with lucite up to 25 cm in depth placed in front of the Molechem detector. At such depths the spectrum was due entirely to electrons created by absorbed Bremsstrahlung radiation.

On the basis of equation (4) page 18 the mean energy of the beam of electrons is expected to decrease linearly with depth in the absorber, and from the data of Table II the most probable energy loss is also expected to decrease, however, the most probable energy loss increased by approximately 10% as the depth of the detector in the phantom increased from 0 to the maximum as shown in Table I. The experimental fluctuations were too great to determine

whether or not the change was linear; however, it was clear that with decreasing energy of the primary electron the most probable energy loss increased significantly. This result was in contrast to the calculations, in which the most probable loss decreased slightly as the electron energy decreased from 35 MeV to 1.5 MeV as shown in Table II. The implication was that the assumptions on which the calculation of the most probable energy loss was based were not completely valid. For instance, W_1 was constant for electrons of energy E from 5 to 35 MeV, and defined the maximum single energy transfer that was to take place on the average just once in the detector. However, the relative number of interactions of energy transfer less than W_1 as compared to the number of interactions of energy transfer greater than W_1 may not have been constant. Then, as the restriction on collisional energy transfers for calculating the restricted stopping power, W_1, did not have the same meaning over the whole range of energies. The restriction must be defined by some other, more sophisticated criterion if the restricted stopping power is to be used to calculat the most probable energy loss.

At large depths the most probable energy loss reached a constant value. The electron spectrum at such depths was determined by the reabsorption of Bremsstrahlung radiation produced at lesser depths. Although the intensity

of Bremsstrahlung decreases with depth, the spectrum of radiation remains fairly constant. Thus the electron spectrum remained relatively constant as well as the energy deposition spectrum.

The increase in the relative number of higher energy deposits with greater depth in an absorber has been noted, and is clearly shown by the shape of the spectra in Figures 9 and 10 and also by the increase in mean energy loss. This increase could be the result of either one, or both, of two effects. The one effect might be that at lower primary energies, e.g. at 5 MeV as opposed to 35 MeV, the relative number of energy losses larger than the most probable energy loss increases.

Another source of depositions of energy greater than the most probable energy loss is electrons with energies greater than the most probable energy loss but less than 1 MeV. The stopping power rises rapidly with decreasing energy when the electron energy is less than 1 MeV, and thus the electron can deposit more energy as it passes through. If the electron energy is less than 380 keV for the ORTEC detector or 230 keV for the Molechem detector, the electron will be completely stopped, thus depositing its total energy. In fact, due to multiple scattering, a significant number of electrons with energies up to a few hundred keV higher than the above listed values can be completely stopped in the detector. Thus the change in

shape of the spectrum with increasing depth may have been due to an increasing number of electrons with energies less than 1 MeV. Such electrons could have been primary electrons reduced to that energy, or secondary electrons produced by the primaries. This latter possibility would agree with Harder's suggestion, mentioned on page 28, that there may be an increase with depth in the number per rad of medium energy secondaries.

The difference between the two possible contributions to the increase in mean energy loss should be emphasized. In the first case, electrons with energies greater than about 1.5 MeV are involved. Such electrons definitely pass through the detector and leave behind only a fraction of their energy. Due to the discontinuous nature of the stopping of an electron there will be a considerable variation in the energy deposited in the detector, but one can define a most probable energy loss. However, the proportion of the electrons that deposit energies in the range of the most probable energy loss may change with energy. The experimental results can be explained if in fact the proportion of electrons depositing the most probable energy increases with electron energy over the range of 1.5 to 35 MeV.

In the second case, electrons with energies less than 1 MeV, but greater than the most probable energy loss, are of interest. These electrons will deposit a large

fraction of their energy up to their total energy. Such deposits will certainly be larger than the most probable energy loss of electrons with energies greater than 1.5 MeV. If in fact there is an increase with depth in the relative number of electrons with energies less than 1 MeV but greater than 125 keV in the ORTEC detector and 60 keV in the Molechem detector, then the experimental results can be explained.

Likely both effects were involved to some extent. However, the question was not resolved in this thesis project. A build-up in the relative number of secondary electrons with energies less than 1 MeV could be of significance in the question of the change of biological effectiveness of electrons with depth in an absorber. If there is a relative increase with depth in the number of electrons per rad with sufficient energy to produce secondaries that are instrumental in initiating a biological change, it follows that there would be an increase with depth in the relative biological effectiveness. It seems thus, that it would be of some value to resolve this question. Some suggestions as to how this might be done are included in the final chapter.

CHAPTER VI

CONCLUSIONS AND SUGGESTIONS FOR FURTHER INVESTIGATION

Topics involved in discussing the energy loss by high energy electrons have been reviewed, with mention of some of the problems that remain to be solved. There are, and will continue to be, technical problems to be overcome in order to improve the monitoring of all radiations. However, the main topics of concern at the present time are those related to the mechanisms by which radiation produces a biological change.

The betatron at The Manitoba Cancer Treatment and Research Foundation has been adapted for use as a source of electrons at an output that will allow analysis of the events associated with individual electrons. The adaptation was relatively simple and the procedures used in this project are described in Appendix B. In general, it seems preferable to monitor the required performance of the betatron by some external means rather than simply to reproduce settings of the controls of the betatron.

Apparatus to operate a semiconductor detector and analyze its output has been assembled. Since most of the equipment was transistorized it worked reliably with very little drift in spite of the fact that it was not used continuously. The calibration could always be

checked at the time of use with test pulses, so that calibration of the system with a reference source was required only once for each detector.

A series of spectra of the energy deposition in two different detectors due to electrons of 35 MeV and 20 MeV energy penetrating different depths of lucite was collected and analyzed. The most probable energy loss is a very prominent feature of these spectra. This most probable energy loss was lower, by as much as 35%, than the loss that would be estimated by multiplying the mean stopping power by the thickness of the detector. If one is concerned with a biological result that is dependent on individual events rather than on the gross energy deposited in a large region, this difference could be important. The use of the mean rate of energy loss times the appropriate distance would produce misleading calculations, since it would neglect the fact that most of the events deposit considerably less energy.

There is a lower limit to the energy which a semiconductor detector and its associated electronic equipment can detect, because of noise that is spontaneously generated by the equipment. This was as high as 45 keV for the Molechem detector under the operating conditions that were used in this project. Under extreme care this noise level might be reduced to about 10 keV with similar equipment. With cooled,

lithium-drifted detectors, noise has been reduced to the order of a few keV, but it appears that this is close to the lower limit for semiconductor detectors with the electronic equipment presently available. Thus it does not appear likely that semiconductor detectors will be of any direct value in answering questions such as those posed by Wideroe: i.e. questions about the density of electrons with energies of the order of 1 keV or less.

With increasing depth of the absorber, there was an increase in the relative number of deposits of energy greater than the most probable energy loss. Two possible reasons for the effect are given. One possibility is that the change is due to a natural shift in the proportion of the energy dissipations by the high energy primaries; the other possibility is that there is a build-up with depth in the relative number of secondary electrons with energies less than 1 MeV. The latter possibility, it has been suggested, would lead to an increase in the relative biological effectiveness with depth.

It is clear that it would be of value to determine which of the above possibilities is producing the observed effect, and to learn more about the distribution of energies deposited by electrons. In this respect it would have been useful to have been able to study the energy deposition

spectra at energies less than the peak of the most probable energy loss distribution. Some information on this topic was available, but the detector broke down before the questions involved could be pursued systematically. Replacement of the ORTEC detector may allow this to be done in the future.

There are several other ways whereby the reasons for the shift in the spectra could be discovered. With no absorber in front of the detector, the spectra due to electrons from 35 MeV down to about 1 MeV could be collected. This would determine the shape of the spectra for primary electrons of these energies. These spectra would then be compared with those obtained due to 35 MeV electrons at depths in the absorber such that the mean energy of the beams corresponded to the primary energy. Although data had been collected at 35 MeV and 20 MeV, the differences were not sufficient to draw any conclusions. Apparently the betatron can be adjusted to produce electrons with energies less than 5 MeV, but some means other than the dials on the control panel would be needed to determine the energy.

On the basis of the Møller cross section for secondary electron production, one should be able to calculate the relative importance of the production of secondary electrons with energies greater than or less

than the value W_1. If this calculation were done for a series of primary electron energies one could determine whether there should be fewer high energy deposits from 35 MeV electrons, than from 5 MeV electrons as the experimental results implied.

Another procedure would be to place a plastic scintillation counter directly behind a semiconductor detector in a transmission mount. Shielding would have to be arranged so that only the electrons that passed straight through the semiconductor detector would be able to get to the scintillating plastic. The plastic should be of sufficient depth to stop a 35 MeV electron. The scintillation counter would then be used to open a coincidence gate whenever electrons within a given energy range were stopped. Pulses from the semiconductor would be delayed slightly and the coincidence gate would be opened to allow their analysis only if they were in coincidence with an electron of the proper energy appearing in the scintillator. By adjusting the coincidence gate to open for different electron energies, the portion of the energy dissipation spectrum due to such electrons could be determined.

Thus it is evident that there are questions associated with the energy loss of high energy electrons, for which semiconductor detectors may be able to supply

some valuable answers.

APPENDIX A

EQUATIONS REQUIRED FOR THEORETICAL CALCULATIONS

The expressions required for calculating the mean stopping power of silicon, the restricted mean stopping power, and other parameters used in Chapter V are presented in this appendix.

A solution for the mean stopping power of matter for relativistic electrons was developed by Bethe on the basis of the Moller formula for the electron-electron scattering cross section. This solution took into account the energy lost by the energetic electron due to collisions with an atomic electron, i.e. an excitation of an atom, an ionization, or the production of an energetic secondary electron. The effects of nuclear scattering and radiative collisions were not included. A common formulation of the above solution is given in Bethe and Ashkin [3]. With the density effect correction of Sternheimer included the expression, written as a mass stopping power, is

$$-\frac{1}{p}\frac{dE}{dx} = \frac{2\pi N_a e^4 Z}{m_o v^2}\left[\ln\frac{m_o v^2 E}{2I^2(1-\beta^2)} - (2\sqrt{1-\beta^2} - 1 + \beta^2)\ln 2 + 1 - \beta^2 + \frac{1}{8}(1-\sqrt{1-\beta^2})^2 - \delta\right] \quad \ldots\ldots (A\text{-}1)$$

where - properties of the incident electron are given by:

E = kinetic energy = total energy - rest mass energy

v = velocity

$\beta = v/c$

m_o = electron rest mass

- properties of the stopping media (with values for Silicon) are:

Z = atomic number (14)

A = atomic weight (28.081 gm/mole)

p = density (2.33 gm/cm^3)

I = mean ionization energy (172 eV)

δ = density effect correction

- other parameters are:

N_a = Avogadro's number = 6.025×10^{23}

e = electron charge = 4.8×10^{-10} e.s.u.

The density of Si was that quoted by the detector manufacturers. The mean ionization energy and density effect correction were evaluated specifically for Si by Sternheimer [50].

To avoid the calculations necessary for a complete table of the energy losses in Si, reference was made to the work of Berger and Seltzer [12]. Using equation (A-1) in a different but equivalent formulation they had tabulated the mass stopping power due to collisional energy losses. By applying equation (A-1) to Si for a few test energies,

it was found that the table for Al, calculated by Berger and Seltzer, could be applied to Si with a simple proportionality factor. The expression

$$\frac{1}{\rho}\frac{dE}{dx}\text{ for Si} = 1.04\,\frac{1}{\rho}\,\frac{dE}{dx}\text{ for Al} \qquad \text{.....(A-2)}$$

was correct within 1% for electrons of energies from 10 keV to 35 MeV.

Berger and Seltzer also included an expression for the restricted stopping power. This expression gave the mean energy loss due to collisions with atomic electrons when only energy transfers less than a specific value were considered. Such information was conveniently expressed in the form of a graph of the value P versus the parameter g; where P was the ratio of the restricted to the unrestricted mean collision loss, and g was the largest fraction of its energy which an electron was allowed to lose in a single collision. For electrons the maximum value for g is 0.5 at which point P has the value 1. At a fixed electron kinetic energy E, P varied linearly with log g. Berger and Seltzer produced this graph for electrons in water. A similar graph for Si was made by determining P for Si at several energies for a fixed value of g. This graph is shown in Figure A-1.

The Moller approximation to the cross section

FIGURE A-1

RATIO OF RESTRICTED TO UNRESTRICTED
MEAN COLLISION LOSS IN SILICON

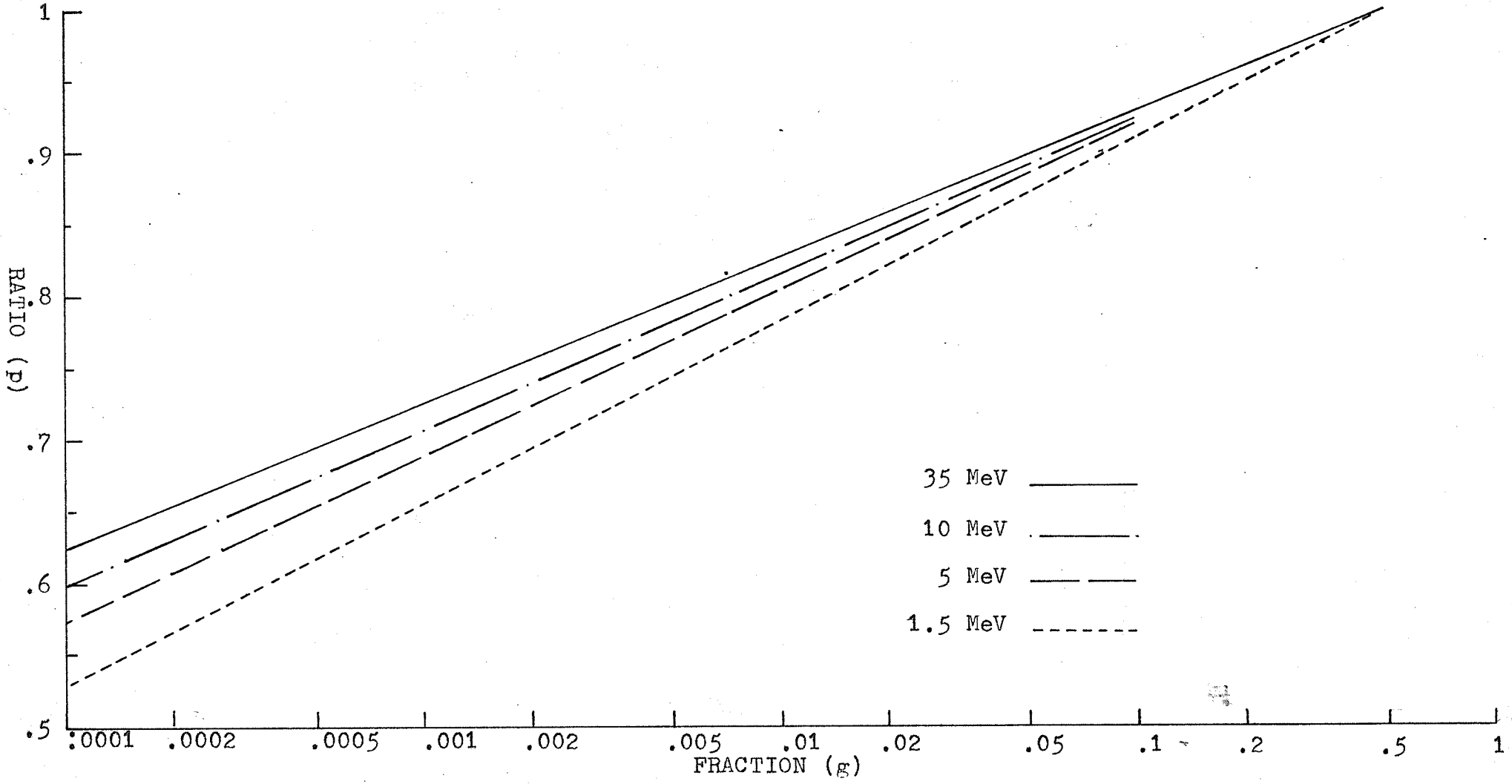

for the production of a secondary electron in a given energy range from a primary electron of relativistic velocity is quoted by Bethe and Ashkin [3]. On the basis of this cross section they introduced a parameter W_1 defined as that individual energy transfer which occurs on the average just once in the distance X over which the energy loss is being observed. The value of this parameter is given by

$$W_1 = 2\pi e^4 \frac{NZX}{mv^2} \qquad \text{(A-3)}$$

where - W_1 is in MeV

- X is the distance of observation in cm.

- N is the number of atoms/cm^3 in the stopping material, i.e. $N = \frac{N_a p}{A}$

  p = density (gms/cm^3), A = (gms/mole) of the material

With the constants of equation (A-3) evaluated for Si; with $v = \beta c$; and with X in cm, W_1 can be calculated in keV from

$$W_1 = \frac{179\ X}{\beta^2}\ \text{keV} \qquad \text{(A-4)}$$

APPENDIX B

OPERATION OF THE BETATRON

In routine operation of the betatron, five controls are adjusted to achieve the desired output. These are the energy, field correction, beta-extraction, contraction, plus coarse and fine phase injection. For normal outputs, a chart is available listing the standard settings of the first three controls, for a given energy. The last two controls are used to tune the betatron to the desired rate of output and maintain that level. However, the normal outputs used in therapy were usually much too high for the special applications of this project. Thus the betatron had to be detuned away from optimum output. Since the output drifted with respect to the various control settings, it was of little use to list the specific settings used during experimentation. It was preferable to define the desired output in terms of some external criteria. The criteria used and the means of attaining it are described in this appendix.

Most often the criterion was an output of 5 to 10 counts per second in the semiconductor detector. Such a low observed counting rate was required due to the pulsed output of the betatron which delivers radiation for a total of only 6×10^{-4} seconds, each second. Thus,

6 counts per second required the electronic equipment to operate at an effective counting rate of 10^4 counts per second during a burst. This rate yielded a sufficient number of events to be analyzed and yet restricted the number of coincident events. At first, turning the filament heating of the betatron injection tube to zero reduced the output considerably. However, it was later suggested by a representative of Brown Boveri that this procedure be avoided if possible. After much trial and error a simple alternative procedure was developed.

The desired energy for the electrons was adjusted by the energy dial and read on the energy meter. The contraction and phase injection were set to the extreme clockwise position, i.e. greater than 100. Then the field correction alone was used to control the level of the output, and the beta-extraction was adjusted so that each burst was spread over as long a period as possible. When no absorber was in front of the detector, the field correction was set around 5. With increasing absorber thickness the field correction was increased up to about 25 to maintain the desired counting rate. For 35 MeV the beta-extraction was set to less than zero and for 20 MeV it was set at 50. An oscilloscope monitoring at the "A.D.C. inspect" of the pulse height analyzer was an invaluable aid in arriving at the desired output from

the betatron.

From the experience of operating the betatron under a variety of conditions during the course of this project, there are some general comments that can be made. It is difficult to obtain a constant, and reproducible, high level of output. Frequent minor adjustments of the tuning controls are required. Output levels much below normal can be obtained but the normal monitoring instruments are insensitive to such levels. Alternate external criteria are required to monitor the output. One criterion has been described above. Another monitor that was used for some purposes was a Faraday Cup attached to a Dynacon Electrometer. Electrons from the betatron were stopped in slug of aluminum in the Faraday Cup and were "counted" in the form of a current as low as 10^{-15} amperes by the electrometer.

BIBLIOGRAPHY

1. J. S. Laughlin, "High-Energy Electron Beams" in Radiation Dosimetry, G. J. Hine & G. L. Brownell, Editors, (Academic Press Inc., New York, 1956)

2. H. E. Johns, The Physics of Radiology, (Thomas, Springfield, Illinois, 1961)

3. H. A. Bethe & J. Ashkin, "Passage of Radiation Through Matter" Part II, in Experimental Nuclear Physics Vol. I, E. Segre, Editor, (John Wiley & Sons, Inc., New York, 1953)

4. R. D. Evans, The Atomic Nucleus, (McGraw-Hill, New York, 1955)

5. R. D. Birkhoff, "The Passage of Fast Electrons Through Matter" in Handbuch der Physik, 34, S. Flügge, Editor, (Springer-Verlag, Berlin, 1958)

6. L. V. Spencer & F. H. Attix, Rad. Res. 3, 239 (1955)

7. P. J. R. Burch, Rad. Res. 3, 361 (1955)

8. R. M. Sternheimer, Phys. Rev. 88, 851 (1952)

9. Ibid., 93, 351 (1954)

10. Ibid., 103, 511 (1956)

11. A. Nelms, "Energy Loss and Range of Electrons & Positrons", N.B.S. Circular 577 (1956) and Supplement to N.B.S. Circular 577 (1958)

12. M. J. Berger & S. M. Seltzer, "Tables of Energy-Losses and Ranges of Electrons and Positrons" Part 10 in Studies in Penetration of Charged Particles in Matter by National Academy of Science-National Research Council, Publication 1133 (1964) (also titled - Nuclear Science Series Report 39)

13. R. T. McGinnies, "Energy Spectrum Resulting from Electron Slowing Down", N.B.S. Circular 597 (1959)

14. L. V. Spencer, "Energy Dissipation by Fast Electrons", N.B.S. Monograph I (1959)

15. International Commission on Radiological Units and Measurements (I.C.R.U.) Report 10 (a) (1962) Radiation Quantities and Units (N.B.S. Handbook 84)

16. W. H. Bragg, Phil. Mag. 20, 385 (1910)

17. L. H. Gray, Proc. Royal Soc. (London) A-122, 647 (1929)

18. Ibid., A-156, 578 (1936)

19. G. C. Laurence, Can. J. Res. A-15, 67 (1937)

20. G. N. Whyte, Nucleonics 12, No. 2, 18 (1954)

21. P. J. R. Burch, Rad. Res. 6, 79 (1957)

22. T. E. Burlin, Phys. Med. & Biol. 6, 33 (1961)

23. Ibid., Vol II, No. 2, 255 (1966)

24. National Committee on Radiation Protection and Measurements (N.C.R.P.), Report No. 27, (1961) Stopping Powers for Use with Cavity Chambers (N.B.S. Handbook 79)

25. D. Harder, Report 1.2.2 in Symposium on High-Energy Electrons, Montreux (Switzerland) Sept. 1964, Edited by A. Zuppinger & G. Poretti (Springer, 1965). (This report is in German and was translated by A. F. Holloway)

26. Ibid., Report 1.1.3

27. J. M. Beattie, K. C. Tsien, J. Ovadia, J. S. Laughlin, Am. J. Roentgenol. 88, 235 (1962)

28. G. W. Dolphin, N. H. Gale & A. L. Bradshaw, Brit. J. Radiol. 32, 13 (1959)

29. N. F. Mott, Proc. Royal Soc. (London) A-126, 259 (1930)

30. C. Møller, Ann. Physik 14, 531 (1932)

31. L. H. Gray, Brit. J. Radiol. Supplement #1, p. 8 (1947)

32. D. V. Cormack & H. E. Johns, Brit. J. Radiol. 25, 369 (1952)

33. R. E. Zirkle, D. F. Marchbank, K. D. Kuck, J. Cell Comp. & Physiol. 39 Supplement #1, 75 (1952)

34. P. J. R. Burch, Rad. Res. 6, 289 (1957)

35. _____, Brit. J. of Radiol. 30, 524 (1957)

36. R. H. Haynes & G. W. Dolphin, Phys. in Med. & Biol. 4, 148 (1959)

37. U. Fano, "A List of Currently Unsolved Problems" Part 12 in A Study of Penetration of Charged Particles in Matter by N.A.S.-N.R.C. Publication 1133 (1964)

38. Report of the R.B.E. Subcommittee to the International Commission on Radiological Protection and the International Commission on Radiation Units and Measurements, Health Physics 9, 357 (1963)

39. W. H. Sinclair & H. J. Kohn, Radiology 82, 800 (1964)

40. A. F. Holloway, A series of unpublished seminars on the topic of R.B.E., presented to staff of the Manitoba Cancer Treatment and Research Foundation, (1965)

41. B. Markus & E. Sticinsky, Strahlentherapie 115, 393 (1961)

42. H. Fritz-Niggli & H. R. Schinz, Strahlentherapie 115, 379 (1961)

43. A. Wambersie, A. Dutreix, J. Dutreix, M. Tubiana, Report 1.4.3 in Symposium on High-Energy Electrons, Montreux (Switzerland) Sept. 1964, Edited by A. Zuppinger & G. Poretti (Springer, 1965)

44. E. P. Malaise, Report 2.2.6, Ibid.

45. R. Loevinger, Report 2.1.11, Ibid.

46. R. Wideroe, Report 2.4.1, Ibid.

47. R. Wideroe, Reports 1.1.4 & 1.2.7, Ibid.

48. J. Ramnath, Unpublished results of the energy calibration of the betatron at the Manitoba Cancer Treatment and Research Foundation, Summer Student Project (1966)

49. R. Loewinger, C. J. Karzmark, M. Weissbluth, Radiology 77, 906 (1961)

50. R. M. Sternheimer, Phys. Rev. 145, 247 (1966)

AN AUTOMATIC ANALOG TO DIGITAL CONVERTER FOR GRAPHICAL RECORDS